Remote Sensing of Environment 161 (2015) 43–62

Contents lists available at ScienceDirect

Remote Sensing of Environment

journal homepage: www.elsevier.com/locate/rse

A global comparison of alternate AMSR2 soil moisture products: Why do they differ?

Seokhyeon Kim [a], Yi.Y. Liu [b], Fiona M. Johnson [a], Robert M. Parinussa [a,c], Ashish Sharma [a,*]

[a] School of Civil and Environmental Engineering, University of New South Wales, Sydney, Australia
[b] ARC Centre of Excellence for Climate Systems Science & Climate Change Research Centre, University of New South Wales, Sydney, Australia
[c] Earth and Climate Cluster, Department of Earth Sciences, VU University Amsterdam, Amsterdam, Netherlands

ARTICLE INFO

Article history:
Received 21 June 2014
Received in revised form 3 February 2015
Accepted 5 February 2015
Available online 19 February 2015

Keywords:
AMSR2
JAXA
LPRM
COSMOS
Soil moisture

ABSTRACT

This study assesses two remotely sensed soil moisture products from the Advanced Microwave Scanning Radiometer 2 (AMSR2), a sensor onboard the Global Change Observation Mission 1 — Water (GCOM-W1) that was launched in May 2012. The soil moisture products were retrieved by the Japan Aerospace Exploration Agency (JAXA) algorithm and the Land Parameter Retrieval Model (LPRM) developed by the VU University Amsterdam, in collaboration with the National Aeronautics and Space Administration (NASA). The two products are compared at the global scale. In addition, the products are evaluated against field measurements from 47 stations from the COsmic-ray Soil Moisture Observing System (COSMOS) network which are located in the United States (36 stations), Australia (7 stations), Europe (2 stations) and Africa (2 stations).

After examining the retrieval algorithms, it is hypothesized that four factors, namely, physical surface temperatures, surface roughness, vegetation and ground soil wetness conditions, may affect the quality of soil moisture retrievals. From the inter-comparisons at the global scale, the correlations of the two products highlight differences in the representation of the seasonal cycle of soil moisture, with negative correlations found for several regions. Correlations of the anomaly time series were generally strong ($R > 0.6$) as a result of soil moisture sensitivity to external meteorological forcing and possibly also random noise in the satellite observations. Due to the inherent differences in spatial coverage and measurement scale of the COSMOS and satellite data, the comparisons in terms of correlation coefficients are the most reliable. It was found that both products show rapid decreases in correlation coefficients under low mean temperature (<290 K), high mean EVI (>0.3) and highly wetted conditions. These findings are further supported by the bias and RMSE estimates which show that JAXA has relatively better performance under dry conditions while the bias and RMSE of LPRM are generally smaller than JAXA, when considered against the four variables. These results provide information on appropriate parameterizations and model selection for the retrieval algorithms and a future research direction to improve the quality by leveraging the strengths of the JAXA and LPRM algorithms. With these, when a multi-year dataset is available, there will be more confidence in defining the seasonal cycle and the data can be decomposed to identify the anomalies where the bias is not relevant.

1. Introduction

Soil moisture is an important variable in hydrological systems affecting the water cycle in the atmosphere, land surface and subsurface. It is considered that microwave remote sensing provides a unique capability for retrieving soil moisture at the global scale (Njoku & Entekhabi, 1996; Schmugge, Kustas, Ritchie, Jackson, & Rango, 2002) and a number of microwave-based soil moisture products have been used in various fields of Earth sciences in the past decades (Brocca et al., 2010; Bruckler & Witono, 1989; Chen, Crow, Starks, & Moriasi, 2011; Crow & Ryu, 2009; Engman, 1991; Jackson, Schmugge, & Engman, 1996; Schmugge et al., 2002; Wagner et al., 2007; Zhu et al., 2014). The primary advantage of microwave-based observations is that they are available under cloudy weather and night time, are less sensitive to roughness conditions of the surface (Wigneron, Schmugge, Chanzy, Calvet, & Kerr, 1998) and can provide information on water content of the top soil layer, rather than the land surface only, even under vegetation coverage (Njoku & Entekhabi, 1996).

To better understand the accuracy of microwave-based soil moisture retrievals, many previous studies have investigated the performance of remotely-sensed soil moisture products by validating against ground-based observations (Albergel et al., 2012; Brocca et al., 2011; Draper, Walker, Steinle, De Jeu, & Holmes, 2009; Gruhier et al., 2010; Jackson et al., 2010; Yee, Walker, Dumedah, Monerris, & Rüdiger, 2013). These studies have concluded with remarks on their relative strengths and

* Corresponding author.
E-mail address: a.sharma@unsw.edu.au (A. Sharma).

http://dx.doi.org/10.1016/j.rse.2015.02.002
0034-4257/

weaknesses among the products by presenting their error statistics such as bias, standard error, root mean squared error (RMSE) and correlations with ground-based measurements. Other ways to evaluate the remotely-sensed soil moisture products at the footprint scale include modern validation techniques such as triple collocation (Crow, Miralles, & Cosh, 2010; Dorigo et al., 2010; Miralles, Crow, & Cosh, 2010; Scipal, Holmes, de Jeu, Naeimi, & Wagner, 2008) and rainfall-based data assimilation verification (Crow et al., 2010).

While microwave can provide near-real time observation (global coverage every 1–3 days for the majority of the sensors), its direct applications have been limited due to the coarse spatial resolution (>100 km^2) and uncertainties resulting from a number of complex factors that affect the radiative transfer model. Due to these complexities, several retrieval algorithms have been developed or are under development to estimate surface soil moisture from microwave emissions (De Jeu & Owe, 2003; Fujii, Koike, & Imaoka, 2009; Jackson, 1993; Koike et al., 2004; Njoku, Koike, Jackson, & Paloscia, 1999; Njoku, Jackson, Lakshmi, Chan, & Nghiem, 2003; Owe, De Jeu, & Walker, 2001; Wigneron, Chanzy, Calvet, & Bruguier, 1995).

The Advanced Microwave Scanning Radiometer 2 (AMSR2) is a passive microwave sensor onboard the Global Change Observation Mission 1 — Water (GCOM-W1) satellite that was launched by the Japan Aerospace Exploration Agency (JAXA) in May 2012. AMSR2 is the successor of the successful Advanced Microwave Scanning Radiometer for the Earth Observing System (AMSR-E, May 2002–October 2011) which was the first passive microwave sensor that was widely used for the retrieval of soil moisture (Koike et al., 2004; Njoku et al., 2003; Paloscia, Macelloni, & Santi, 2006). AMSR-E provided a number of consistent and continuous datasets for almost a decade. AMSR2 is expected to provide improved spatial resolution due to its larger reflector compared to its predecessor. Moreover, it has an additional 7.3 GHz channel that was developed for Radio Frequency Interference (RFI) mitigation and an improved calibration system (Imaoka et al., 2010). JAXA developed a soil moisture retrieval algorithm (Fujii et al., 2009) and has made available its soil moisture product from AMSR2 since July 2012. Recently, another algorithm, the Land Parameter Retrieval Model (LPRM), developed by the VU University Amsterdam in collaboration with the National Aeronautics and Space Administration (Owe, De Jeu, & Holmes, 2008), has been applied to AMSR2 passive microwave observations to derive a soil moisture product (Parinussa, Holmes, Wanders, Dorigo, & De Jeu, in press). Apart from the soil moisture product, LPRM also produces land surface temperature and vegetation optical depth (VOD) an indicator of the total vegetation water content of above-ground biomass (Liu, de Jeu, McCabe, Evans, & van Dijk, 2011; Liu, van Dijk, McCabe, Evans, & de Jeu, 2013).

Given that the underlying microwave emission observations are the same for LPRM and JAXA retrieval algorithms, an exciting opportunity is now available to assess the effects of algorithms on the resulting AMSR2 soil moisture products. A preliminary correlation analysis between daily LPRM and JAXA soil moisture products for one year at the global scale shows that there are a number of similarities and also differences between these products (Fig. 1).

This paper seeks to answer the obvious question that arises from Fig. 1 — what are the reasons for their similarities and differences? Previous studies have compared individual remotely sensed soil moisture product to ground-based measurements at a regional (Brocca et al., 2011; Draper et al., 2009; Gruhier et al., 2010; Yee et al., 2013) or global scale (Albergel et al., 2012; Albergel et al., 2013; Al-Yaari et al., 2014). These performance verifications have generally been limited to examining differences with little attention paid in identifying the causes for these differences. The objectives of this paper are twofold. First is to provide a guidance for users of these products by performing a comprehensive comparison between these two AMSR2 soil moisture products as well as with ground-based measurements for a single year. The second aim is to identify the reasons for the differences and similarities between the two remotely sensed products for better understanding and further improvements of the algorithms. While JAXA and LPRM algorithms start from the simple radiative transfer model (Mo, Choudhury, Schmugge, Wang, & Jackson, 1982), they use different ways to define the physical surface temperature, surface roughness, vegetation conditions and dielectric constants. The influences of these four factors will be investigated in detail.

More details of the JAXA and LPRM AMSR2 products, ground soil moisture measurements and statistical methods used in this study are described in Section 2. The results of the spatio-temporal comparisons are presented in Section 3 with an emphasis on the regions or time periods where these two products differ. The last sections discuss the results and suggestions for future research directions.

2. Data and methods

Datasets used over the study period 1 August 2012 through 31 July 2013 are listed in Table 1, including: (1) two AMSR2 soil moisture products (JAXA and LPRM algorithms), (2) field soil moisture measurements collected from the COSMOS network, (3) enhanced vegetation index (EVI) from the Moderate Resolution Imaging Spectroradiometer (MODIS) to represent global green vegetation density, (4) topographic data from the Global Land One-kilometre Base Elevation (GLOBE) Digital Elevation Model (DEM), version 1.0

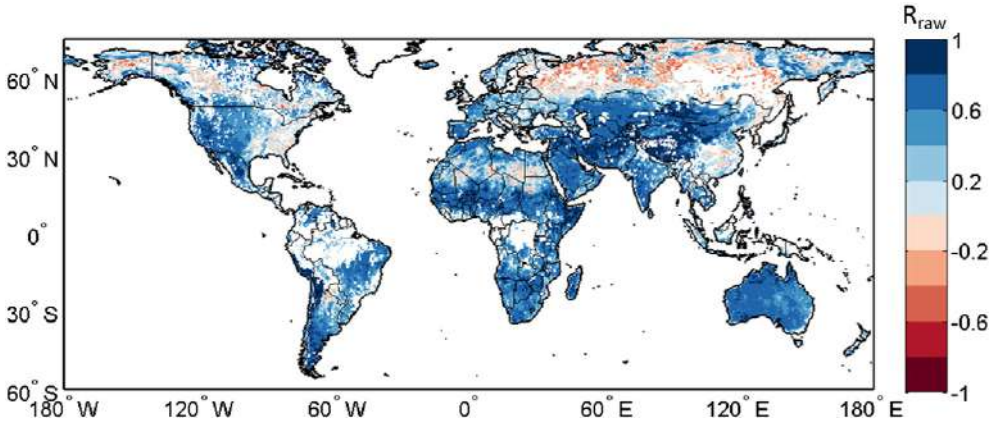

Fig. 1. Spatial distribution of Pearson correlation coefficients (R) between daily JAXA and LPRM soil moisture products for the period August 2012 through July 2013. The soil moisture products are from the descending overpasses of 10.7 GHz (X-band), and the regions with dense forests are masked out.

Table 1
Details of satellite-derived soil moisture, field soil moisture measurements and ancillary data used in this study.

Data	Product name	Temporal resolution	Spatial resolution	Units
AMSR2-JAXA	Level 3 geophysical parameter SMC	Daily	0.25°	m^3/m^3
AMSR2-LPRM	Level 3 Surface Soil Moisture	Daily	0.25°	m^3/m^3
COSMOS	Level 3 SM12H	Hourly	A few hundred metres	m^3/m^3
USCRN	SOIL_MOISTURE_5_DAILY (depth 5 cm)	Hourly	Point measurement	m^3/m^3
MODIS-EVI	MOD13C2	Monthly	0.25° (resampled)	–
Digital Elevation Model	Global Land One-kilometre Base Elevation (GLOBE) Digital Elevation Model, Version 1.0	–	0.25° (resampled)	–
Soil temperature	European Centre for Medium-Range Weather Forecasts (ECMWF) re-analysis (ERA) interim, Soil Temperature Level 1	6 hourly	0.25°	K
Precipitation	Tropical Rainfall Measuring Mission (TRMM), 3-hourly product 3B42 (V7)	Daily (aggregated)	0.25°	mm/day

(GLOBE-Task-Team & Others, 1999) used as an indicator of the large-scale surface roughness, (5) soil temperature level 1 data from ERA-Interim produced by the European Centre for Medium-Range Weather Forecasts (ECMWF) (Dee et al., 2011) to mask out data with freezing condition and (6) precipitation data from Tropical Rainfall Measuring Mission (TRMM 3B42 V7, http://pmm.nasa.gov/node/158) (Huffman & Bolvin, 2014) for qualitative comparisons with the temporal dynamics of the satellite soil moisture products.

2.1. Satellite-based soil moisture products

The LPRM product provides AMSR2 soil moisture retrievals for the 6.9, 7.3 and 10.7 GHz channels as this algorithm can be applied to low microwave frequencies (<20 GHz), whereas the JAXA product is only available for 10.7 GHz. Although the soil moisture retrievals from lower microwave frequencies are expected to be more accurate (Parinussa, Meesters, et al., 2011) this study focuses on the soil moisture retrievals from 10.7 GHz at a 0.25° global grid that is available from both retrieval algorithms. Another benefit is that RFI issues are less severe for the 10.7 GHz soil moisture retrievals than the 6.9 GHz (Njoku, Ashcroft, Chan, & Li, 2005). Differences are noted between ascending and descending overpass soil moisture retrievals (Draper et al., 2009; Fujii et al., 2009; Owe et al., 2001) as the geophysical conditions are different at day- and night-times. As nighttime has more favourable conditions (De Jeu et al., 2008), only soil moisture products from descending overpasses are used in the main text, while results from the ascending overpass data are presented in Appendix C.

Both JAXA and LPRM algorithms use a simple radiative transfer model (Mo et al., 1982) as the starting point. The satellite observed brightness temperature (T_b) measures the natural microwave emissions from the land surface and consists of three components: (1) radiation from the soil attenuated by the overlaying vegetation layer, (2) upward radiation from the vegetation layer and (3) downward radiation from the vegetation, reflected upward by the soil and again weakened by the vegetation canopy (Owe et al., 2001). Both algorithms use brightness temperature at 10.7 GHz and 36.5 GHz channels from AMSR2, but they have differences in estimating physical surface temperature, surface roughness, vegetation dynamics and dielectric mixing models. These four key differences between the two algorithms in relation to the parameterization models are summarized in Table 2 and the section below is dedicated to explaining their differences. Full details about these two retrieval algorithms can be found in Koike et al. (2004) and Fujii et al. (2009) for JAXA and Meesters, De Jeu, and Owe (2005) and Owe et al. (2001, 2008) for the LPRM algorithm.

1. Physical surface temperature: Both JAXA and LPRM algorithms assume that soil temperature (T_s) and vegetation canopy temperature (T_c) are equal. The JAXA algorithm also assumes they are at a constant value of 293 K throughout the year globally (Koike, 2013), whereas the LPRM algorithm estimates the surface temperature based on a linear relationship between vertical polarization T_b at 36.5 GHz and surface temperature as the first step in the LPRM algorithm (Parinussa, Holmes, Yilmaz, & Crow, 2011). Thus the surface temperature is observation-based and dynamic in the LPRM algorithm while constant in the JAXA algorithm.
2. Surface roughness: Both JAXA and LPRM algorithms consider that the emissivity is related to the surface roughness, but different assumptions are made in the way that surface roughness is defined. The JAXA algorithm determined its roughness parameterization for 10.7 GHz and 36.5 GHz through comparing the T_b data observed by passive microwave instrument with in situ data at the Mongolia validation site. The LPRM algorithm used an 'educated guess' based on previous research (Njoku & Li, 1999). For both algorithms the surface roughness is assumed to be constant, but different values are adopted in JAXA and LPRM.
3. Vegetation: The JAXA algorithm is essentially a look-up table method where a linear relationship between optical depth (τ) and vegetation water content (W_c) is applied based on Jackson and Schmugge (1991). The look-up tables are established in advance by simulating T_b at 10.7 GHz and 36.5 GHz corresponding to different combinations of (1) soil moisture (range of 0–0.6 m^3/m^3), (2) vegetation water content (range of 0–1.8 kg/m^2), (3) fractional vegetation cover (f_c, range of 1–100%) and (4) fixed soil and vegetation canopy physical temperature. When a new satellite-observed T_b is collected, two T_b based indices, Polarization Index (PI) (Paloscia & Pampaloni, 1988) and Index of Soil Wetness (ISW) (Koike, Tsukamoto, Kumakura, & Lu, 1996) are calculated. PI is obtained by dividing the T_b difference between vertical and horizontal polarizations at

Table 2
Summary of main differences between JAXA and LPRM algorithms.

Parameter	JAXA	LPRM
Soil and vegetation canopy physical temperatures	$T_s = T_c = 293$ K	$T_s = T_c$, linearly related with $T_{b(37\ GHz[V])}$
Surface roughness	Constants Q and H	Constants h and Q
Vegetation	$\tau = b \cdot W_c$ $f_c = f(\mathrm{NDVI})$ $\omega = 0.060$–0.063 depending on polarization and frequency	$\tau = f(\mathrm{MPDI}, k, u, \omega)$ $\omega = 0.060$
Dielectric mixing model	Four-stream fast model (Liu, 1998)	Wang and Schmugge (1980)

T_s: soil surface temperature, T_c: vegetation canopy temperature, Q: polarization mixing ratio, H and h: roughness parameters used in JAXA and LPRM, τ: optical depth, W_c: vegetation water content, b: vegetation parameter, f_c: fractional vegetation coverage, k: dielectric constant, u: incidence angle, ω: single scattering albedo.

10.7 GHz by their mean values, while ISW is obtained by dividing the T_b difference between 36.5 GHz and 10.7 GHz at horizontal polarization by their mean value. Next, the value for f_c is determined from the MODIS Normalized Difference Vegetation Index (NDVI), and the correct look-up table is selected for that particular f_c, date and location. The soil moisture and vegetation water content values from the selected look-up table are considered as the retrievals. As a result the simulated T_b matches the observed PI and ISW.

The LPRM algorithm retrieves τ differently with the important differences being that no pre-established look-up tables are used and no ancillary vegetation information from optical sensor is required. τ is expressed in terms of mixed dielectric constant (k), incidence angle (u) and the Microwave Polarization Difference Index (Meesters et al., 2005) which is defined as the ratio between the difference of T_b at 10.7 GHz from both polarizations and their sum (Becker & Choudhury, 1988). The soil moisture and τ value are considered as the final retrievals when the difference between simulated and observed horizontal polarization T_b at 10.7 GHz is minimized.

4. Dielectric mixing model: Different dielectric mixing models are used in JAXA and LPRM algorithms (see Table 2). The Wang and Schmugge (1980) model is used in the LPRM algorithm to convert the mixed dielectric constant to a soil moisture value. As the radiative transfer within the soil layer (rather than the soil surface) plays an important role under dry conditions (soil moisture less than 0.1 m^3/m^3), a four-stream fast model (Liu, 1998) that combines the soil radiative transfer model with the conventional soil surface model is adopted in the JAXA algorithm. With increasing soil moisture, the effect of the soil layer disappears and the effect of radiation of the soil surface becomes dominant.

2.2. Field soil moisture measurements

The cosmic-ray method is a newly developed way to measure soil moisture representative of an area of a few hectares and to a depth in the order of a few hundred millimetres in the COsmic-ray Soil Moisture Observing System (COSMOS) (Zreda et al., 2012). Stationary cosmic-ray probes detect neutrons generated by cosmic rays in air, soil and other materials. The neutrons are mainly moderated by hydrogen atoms which are primarily located in soil water, and emitted to the atmosphere in which they are instantaneously mixed within a few hundred metres and the density is inversely correlated with soil moisture (Zreda et al., 2012). At present, 95 COSMOS stations are in operation providing hourly soil moisture data; 68% of them are in the United States with the remainder in Europe, Africa, South America and Australia. Two types of data are available: (1) soil moisture for the counting time interval (1 h) in volumetric units, and (2) a 12-hour running average by using the 12-hour robust boxcar filter to reduce the noise (Zreda et al., 2012) from the International Soil moisture Network (ISMN, http://ismn.geo.tuwien.ac.at/ismn/) (Dorigo et al., 2011) and which is used in this study.

The use of the COSMOS over different continents ensures consistency in measurement techniques and is expected to minimize the uncertainties associated with ground measurements which use various probe types, settings and methods over different regions. Additionally, COSMOS data is expected to provide an area-representative value for soil moisture heterogeneities which can be observed in point measurements within a footprint of the cosmic-ray probe (Zreda et al., 2012).

Nevertheless, one known issue with cosmic-ray derived soil moisture is its uncertainties under high atmospheric water vapour (Zreda et al., 2012). Previous research has investigated the extent of the problem and has suggested corrections with respect to the atmospheric water vapour (Bogena, Huisman, Baatz, Hendricks Franssen, & Vereecken, 2013; Rosolem et al., 2013). To avoid possible errors in this study from the COSMOS data a well-tested quality control (QC) procedure (Dorigo et al., 2013) has been applied, which detects unnatural increases or decreases in soil moisture and flags for those potentially doubtful observations. In this study, all flagged soil moisture values are excluded from further analysis. Accordingly, the final dataset includes field measurements from 47 stations which have at least 6 months overlapping with the satellite observations were used.

As another way of validating the COSMOS data, soil moisture measurements (soil layer depth 5 cm) from 17 stations in U.S. Climate Reference Network (USCRN) (Diamond et al., 2013) are compared to COSMOS datasets when one or more USCRN stations are located within 50 km (i.e. adjacent grids) of the COSMOS stations (see Fig. 2 and Table S1 in the Supplementary data). The results suggest that the temporal patterns of soil moisture measurements between these COSMOS and traditional ground stations are well correlated and provide additional confidence in the comparisons with AMSR2. In spite of the advantages of COSMOS data: the consistency in measurement techniques and the wider horizontal coverage compared to point measurements, it should be noted that the difference in the measurement depths of the cosmic ray probes and the satellite derived soil moisture products still remains a limit just like all studies validating remotely sensed soil moisture, which use in-situ measurements as a reference. It is therefore appropriate to consider the discrepancies in absolute values of the two products,

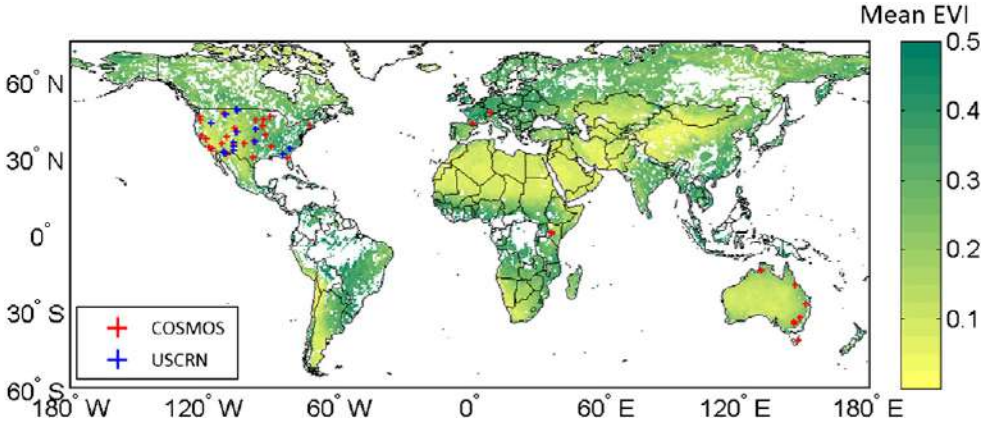

Fig. 2. Locations of 47 COSMOS stations used in this study and coexisting 17 USCRN stations, presented with red and blue '+' symbols respectively. The background colour indicates annual average EVI during the entire study period.

which are represented by bias and root mean square error in this study, as supportive metrics. However, it should be also noted that temporal correlations are not affected by the depth discrepancy problem and therefore the main conclusions in this work rely on the correlations.

The field measurement from each COSMOS station is compared with the satellite-based soil moisture grid cell in which the station is located. When more than one station is located in the same grid cell, their average is taken first. As the satellite observation is a snapshot at the overpass time (0130 equatorial local crossing time for AMSR2 descending overpass), the field measurement recorded at a time closest to the local overpass time is used for a more direct comparison.

2.3. Ancillary data

The MODIS-based enhanced vegetation index (EVI) provides information about global green vegetation conditions. In this study, the original monthly 0.05° resolution EVI product (MOD13C2) was aggregated to 0.25° by taking the average value of 25 0.05° grid cells in each 0.25° grid cell and used as an indication for the vegetation condition at each site.

As an indication for surface roughness at the remotely sensed soil moisture scale (0.25°), the Global Land One-kilometre Base Elevation Digital Elevation Model (GLOBE DEM version 1.0) (GLOBE-Task-Team et al., 1999) was used. In each 0.25° grid cell, there are 625 1 km DEM grid cells. An indication of the relative surface roughness of each 0.25° grid cell is estimated as the variance (σ^2) of elevations from all 625 1 km-DEM grid cells (Choudhury, Schmugge, Chang, & Newton, 1979). The spatial distribution of surface roughness values at the global scale can be found in Fig. B1. This surface roughness proxy is then compared to the errors in soil moisture retrievals for each COSMOS station to test the hypothesis that the differences in the two products' algorithms for surface roughness will lead to changes in the estimates of soil moisture. Although this surface roughness proxy does not exactly represent the overall surface roughness affecting the microwave emission, this simplified investigation provides information on the relationship between surface roughness and the retrieval algorithms' performance. A global map showing the coarse scale surface roughness (log (h)) is included in Appendix B (Fig. B1).

To evaluate the temporal dynamics of the satellite-based soil moisture products, the 3-hourly precipitation product (3B42 V7) from the Tropical Rainfall Measuring Mission (TRMM, http://pmm.nasa.gov/node/158) (Huffman & Bolvin, 2014) was aggregated to daily total precipitation (mm/day). This information can assist in interpreting in particular the anomaly time series of soil moisture where the responses of both products are expected to be influenced by local rainfall.

It is not possible to retrieve soil moisture under frozen conditions. LPRM applies an internal soil-freezing step in the product (Parinussa, Holmes, et al., 2011) whereas the JAXA algorithm provides data under such conditions. Therefore to ensure consistent comparisons between the two products, a mask to remove estimates under frozen conditions has been used. To construct the mask 6-hourly soil temperature of the top-layer (i.e. 0–0.07 m) from the ERA-Interim reanalysis produced by the European Centre for Medium-Range Weather Forecasts (ECMWF, http://data-portal.ecmwf.int) (Dee et al., 2011) was adopted. Since the original soil temperature data is on the Universal Time Coordinated (UTC) time, they were first converted to local time based on station coordinates. Then temporal interpolation was performed between two adjacent temperature values to obtain soil temperature values at the overpass time. When the interpolated ERA-Interim soil temperature is below 0 °C, the corresponding satellite-based soil moisture retrievals, field soil moisture measurements, VOD and EVI were masked out. Other masks that were applied to the data included removing grid cells along the coastline (i.e. centre of grid cells within 25 km from the coast) to remove the influence of ocean water. Regions with dense vegetation (i.e. annual mean VOD greater than 0.8 at 6.9 GHz derived from the LPRM algorithm) are also excluded in this analysis (De Jeu et al., 2008).

2.4. Statistical metrics

The AMSR2 products were evaluated by comparing the two products to each other as well as comparing them to the ground-based soil moisture measurements. The temporal correlations between JAXA and LPRM products were examined over all grid cells for both raw data and anomaly data. The anomaly data was obtained in two steps. The first step was to calculate the seasonal cycle by taking a 31-day moving average over the study period 1 August 2012 through 31 July 2013, while the data actually used is from mid-July 2012 through mid-August 2013. The anomaly data was calculated by removing the seasonal cycle from the raw data. Future work should be carried out using multi-year climatology as more data becomes available. It should also be noted that the 1-year analysis period does not allow conclusions on inter-annual variations and this could be a topic of interest for the future. The seasonal cycles and anomaly time series from each product were compared over all grid cells by considering their correlations as well as the maximum, minimum and mean values.

At each grid cell a paired Student's t-test was used with the daily time series to test the differences in the mean of JAXA and LPRM soil moisture products, with a significance level of $\alpha = 0.05$ adopted for this test. To compare the satellite-based soil moisture and ground-based soil moisture, three statistical metrics were used, namely, the Pearson correlation coefficient, bias and root mean square error (RMSE).

3. Results

3.1. Inter-comparison of JAXA and LPRM products; how are they different?

The spatial patterns of mean, maximum and minimum values of JAXA and LPRM soil moisture products and their difference are presented in Fig. 3. The mean values of JAXA are generally lower than LPRM. Over the high latitude regions, e.g. Russia and Canada, both maximum and minimum values of JAXA products are lower than LPRM, which results in the lower mean values. Over the other regions (except desert regions), the minimum values of JAXA and LPRM are quite similar. The lower mean values of the JAXA product are primarily caused by its lower maximum values. This may be related to the fact that the soil moisture range in the JAXA and LPRM algorithms is 0–0.6 and 0–1 m^3/m^3, respectively. The maximum value (0.6 m^3/m^3) of the JAXA product is a result of the pre-established lookup tables that match soil moisture and vegetation water content to microwave brightness temperature-derived indices (i.e. PI and ISW see Section 2.1). The minimum values of the JAXA product over the desert regions (e.g. Sahara, Africa, Middle East, south Mongolia and central Australia) are somewhat higher than LPRM. This can be attributed to the particular approach used in JAXA to estimate the soil moisture under extreme dry conditions (<0.1 m^3/m^3) as described in Section 2.1. With these considerable differences in the absolute values between these two products, it is not surprising to see that the paired-t test indicates that the means of the two products are statistically different for nearly all grid cells (Fig. A1).

The signals in soil moisture products can be decomposed into the (1) seasonal cycle and (2) soil moisture anomalies which primarily represent responses to rainfall events. The correlation coefficients of the seasonal cycle and anomalies between the two AMSR2 soil moisture products are presented in Fig. 4. The soil moisture anomalies of the two products are highly positively correlated (Fig. 4a) as a result of similar responses to external meteorological forcing and to some extent the same random noise in the satellite observations.

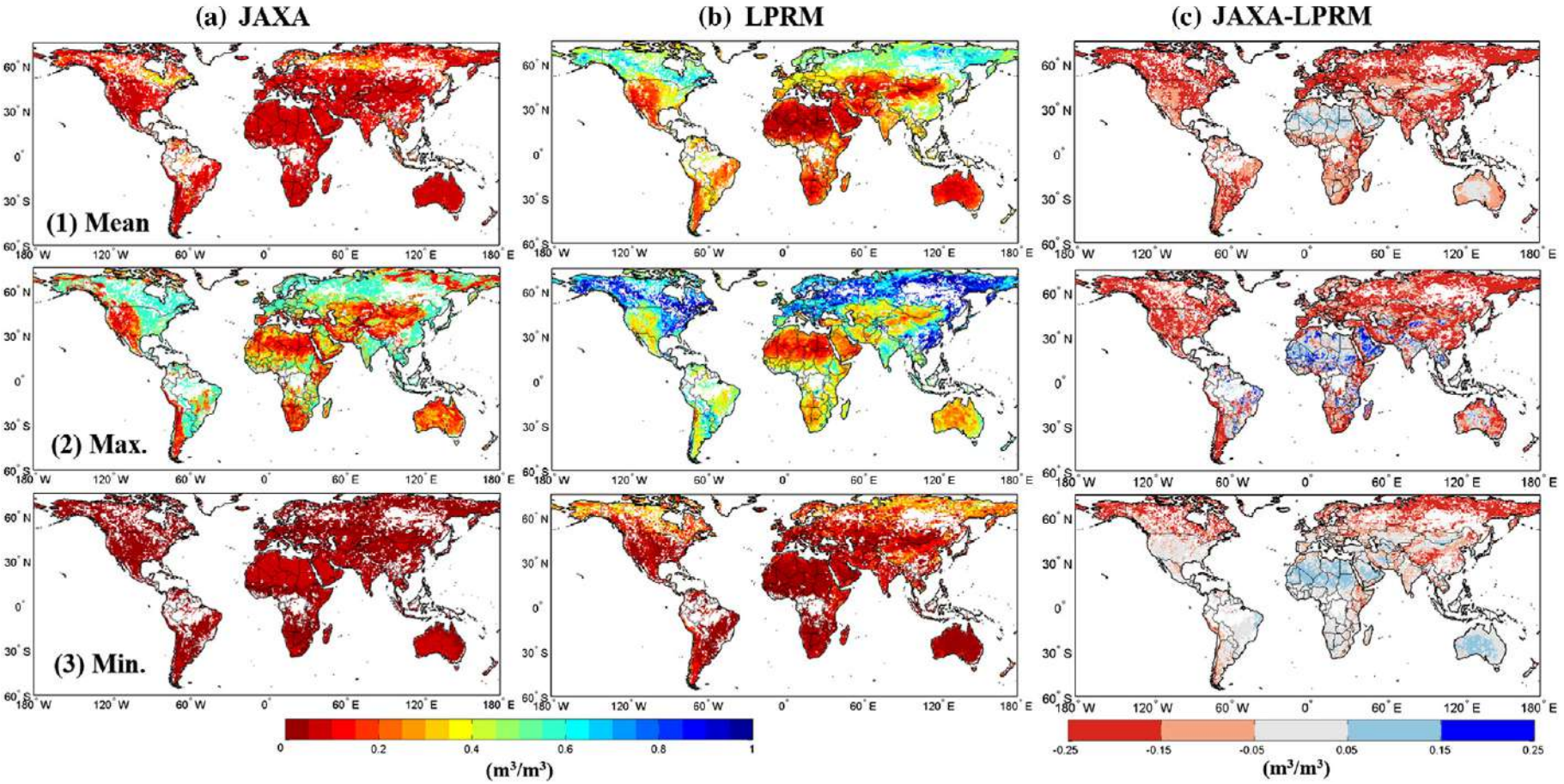

Fig. 3. Global maps of mean (top panels), maximum (middle panels) and minimum (bottom panels) values of JAXA (left column), LPRM (middle column) and differences (i.e. JAXA–LPRM, right column) derived from descending overpasses.

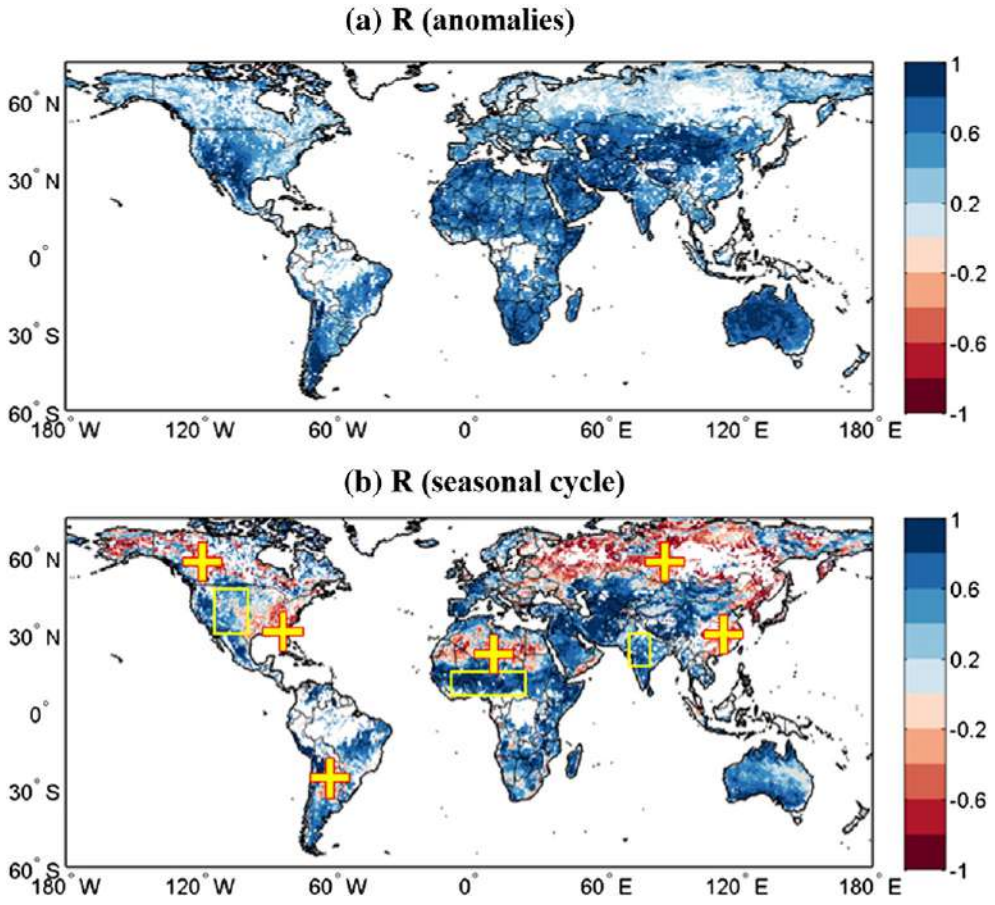

Fig. 4. Global maps of correlation coefficients (R) between JAXA and LPRM soil moisture products derived from descending overpasses for (a) soil moisture anomalies ($R_{anomaly}$) and (b) seasonal cycle (R_{season}). Three regions with strong positive correlations in seasonal cycle (outlined by yellow boxes) are in the transition zones identified by Koster et al. (2004). Six regions with strong negative correlations (labelled as yellow crosses) are selected for further temporal comparison.

Over the 'transitional regions' where strong coupling between soil moisture and precipitation is expected, e.g. central Great Plains of North America, Sahel and India (Koster et al., 2004), both seasonal cycle and soil moisture anomalies are highly positively correlated between these two AMSR2 products (regions highlighted with yellow boxes in Fig. 4b). Strong negative correlation coefficients in seasonal cycles are also found over many regions, e.g. western Canada, Russia, southeast USA, southeast China, central South America and northern Africa (Fig. 4b) Again, it should be noted that the 1 year timeframe in which the products were evaluated does not allow conclusions on inter-annual variations and there will be more confidence in the seasonal cycle results in future when a multi-year climatology can be constructed.

To better understand their temporal characteristics, time series of the JAXA soil moisture and LPRM soil moisture together with soil temperature and EVI over the highlighted regions in Fig. 4b are shown in Figs. 5 and 6. Over the transition regions, the overall correlations during the study period are high and the temporal dynamics as responses to precipitation events are very similar (Fig. 5). However, the recession patterns since the end of wet season are quite different between these two AMSR2 products. Over the Sahel region (Fig. 5b and c), the JAXA soil moisture drops to its lowest value very quickly at the end of wet season and remains constant throughout the following dry season, but the LPRM soil moisture declines gradually. When there is no precipitation event, the temporal patterns of the LPRM soil moisture have a tendency to be opposite to surface temperature. The apparent difference between these two AMSR2 products under the very dry conditions may also come from their different dielectric mixing models. It is noticeable that the EVI value over India is similar between dry and wet seasons (Fig. 5d). Meanwhile, the LPRM soil moisture is kept to 0.3 m^3/m^3 in the dry period whereas the JAXA soil moisture drops to 0.1 m^3/m^3.

Over the regions where strong negative correlations in seasonal cycles are observed, it appears that JAXA soil moisture variations are generally in phase with temperature at the locations with strong seasonal cycles in temperature (Fig. 6a–d). In contrast, the seasonal cycle of the LPRM soil moisture tends to be opposite to the JAXA product and temperature. When the temperature is consistently high (e.g. Fig. 6e South America), the JAXA soil moisture still has a strong seasonal cycle which is similar to the EVI temporal pattern. Meanwhile, the LPRM soil moisture drops sharply with increases in EVI in austral summer (i.e. late 2012 to early 2013). Over the arid Sahara (Fig. 6f) with low EVI during the whole year, there are no notable variations in the JAXA soil moisture during the whole period, while the LPRM soil moisture increases during the rainy season.

The above observations suggest that over these regions where JAXA soil moisture and LPRM soil moisture have opposite seasonal cycles, the dynamics of the JAXA soil moisture agrees with temperature and/or EVI variations whereas the seasonal cycle of the LPRM soil moisture is inversely related to temperature and seems to be considerably affected when vegetation density (represented by EVI) is high which is in line with the findings in Parinussa, Meesters, et al. (2011). It can also be seen in Fig. 6e that when EVI is high in the austral summer the behaviour of JAXA and LPRM is quite different. The performance of the AMSR2

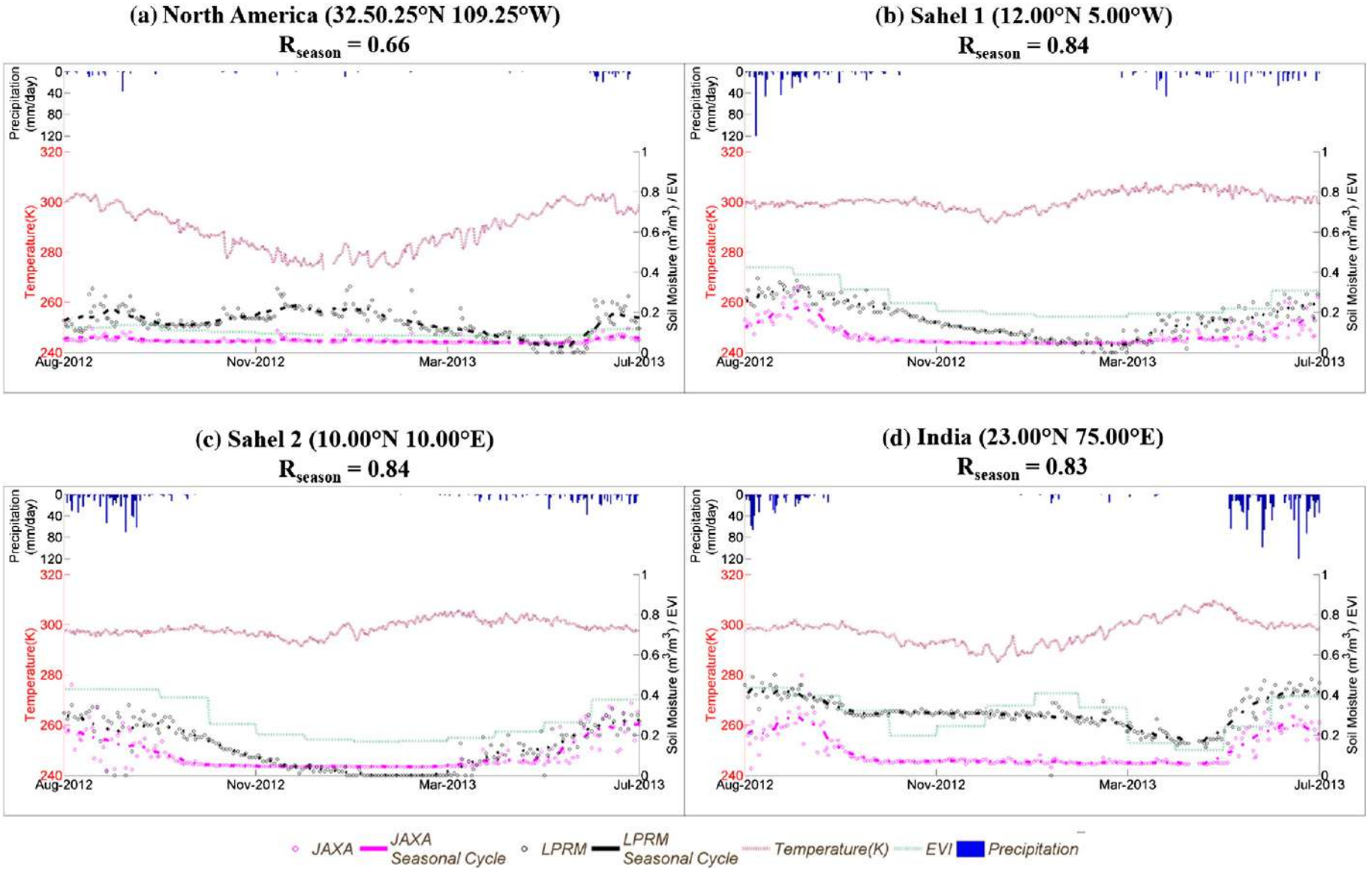

Fig. 5. Descending pass time series of JAXA, LPRM, temperature and EVI at four locations in the transition zones that have strong positive correlations in the representation of the seasonal cycle; (a) the central Great Plains of North America, (b) and (c) Sahel, and (d) India.

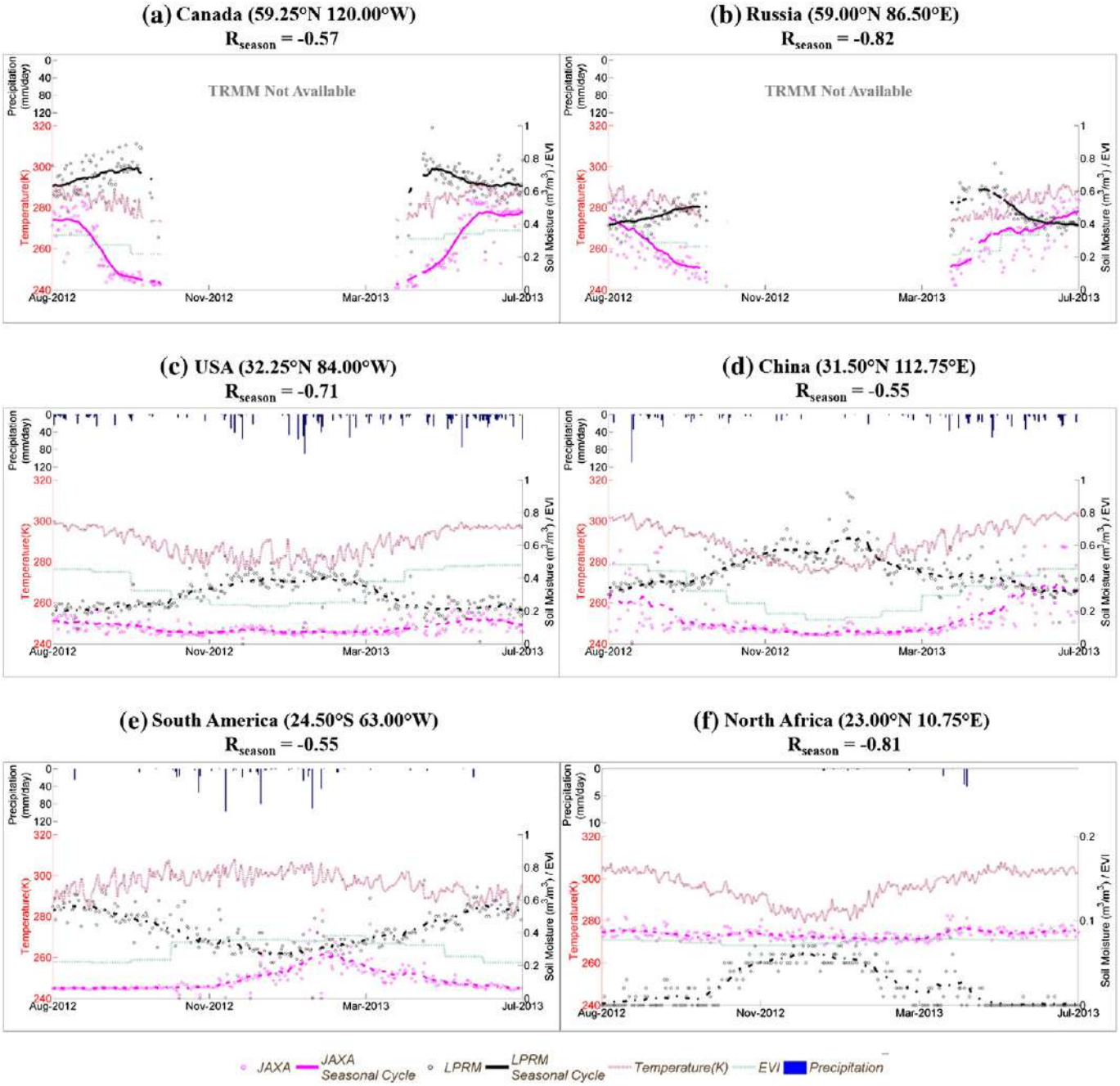

Fig. 6. Time series of JAXA, LPRM, temperature and EVI at six locations that have strong negative correlations in the representation of the seasonal cycle; (a) Canada, (b) Russia, (c) the USA, (d) China, (e) South America and (f) North Africa. Different scales on y-axis are used in panel f for better visualization.

products and vegetation is examined in more detail in the next section for all COSMOS stations to determine if a threshold when EVI affects soil moisture can been found.

3.2. Comparisons against field measurements

For the grid cells with particularly high correlations and those with low or even negative correlations between JAXA and LPRM, both products are compared to field measurements using the available COSMOS stations over the USA (http://cosmos.hwr.arizona.edu/Probes/StationDat/). The USA was selected as it has one of the transition zones identified by Koster et al. (2004) and also has areas where the two products have similar and different seasonal cycles.

At the grid cells with good agreement in the seasonal cycle (Fig. 7 and Table S1), LPRM soil moisture estimates are generally higher than the JAXA estimates, except for the dry season at Santa Rita Creosote (Fig. 7e). The LPRM soil moisture has strong variations throughout the year, while the JAXA soil moisture shows little variation with a similar minimum value around 0.05 m^3/m^3 in the dry season for all four locations. Furthermore, LPRM soil moisture retrievals follow the temporal patterns captured by the ground-based measurements better than JAXA soil moisture retrievals.

When it comes to the grid cells with strong negative correlations in the seasonal cycle (Fig. 8 and Table S1), it is worthwhile to highlight several points here. (1) These stations are located in forested areas and the mean EVI and VOD values are higher than the average value

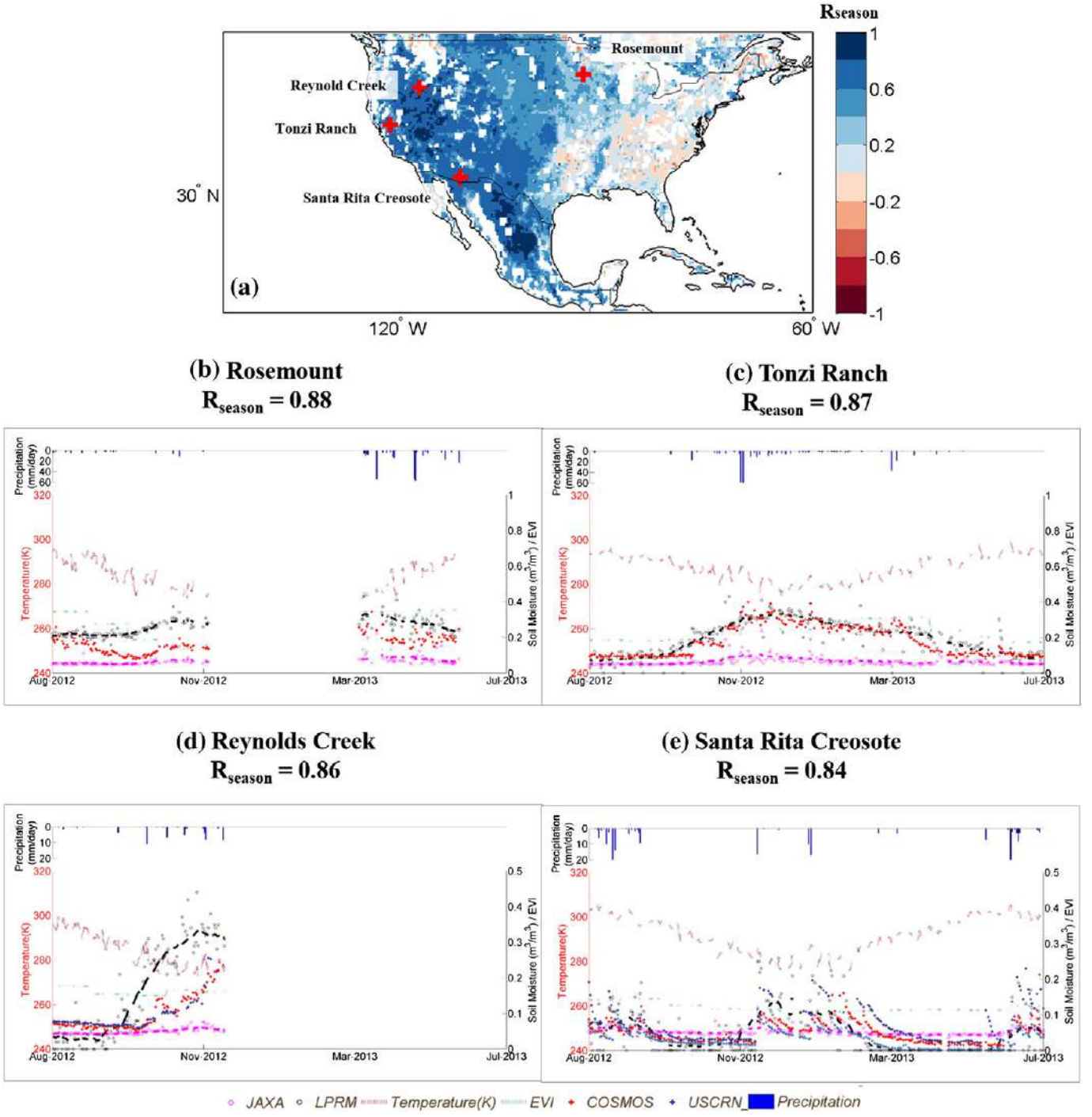

Fig. 7. Time series of AMSR2 soil moisture retrievals, soil temperature, EVI, precipitation and ground soil moisture measurements for four COSMOS stations where R_{season} between JAXA and LPRM product is highest among all grid cells with COSMOS stations. Panel a shows the location of these four stations and R_{season} in the background. Different scales on y-axis are used in panels d and e for better visualization.

of all 47 COSMOS stations used in this study. (2) The dynamics of LPRM products tend to be opposite to field measurements and/or JAXA products (i.e. Savannah River which has the highest mean VOD among them). (3) LPRM soil moisture values tend to be higher than JAXA, which is consistent with the global mean values shown in Fig. 3. (4) It appears that the variance of the LPRM soil moisture product is much larger than the JAXA soil moisture, as the former has much more scatter around the seasonal cycle compared to the latter. (5) At Savannah River and JERC station which are in relatively dry conditions, the JAXA product shows fairly good correspondences to the field measurements. It has been previously found that the LPRM product has difficulties in this region (Hain, Crow, Mecikalski, Anderson, & Holmes, 2011).

Expanding the comparisons from the 8 stations included in Figs. 7 and 8, the error statistics at all 47 COSMOS stations are now considered. For each station the error statistics (bias, RMSE and R) between both AMSR2 products and ground-based measurements are plotted against four independent variables, namely, annual mean temperature,

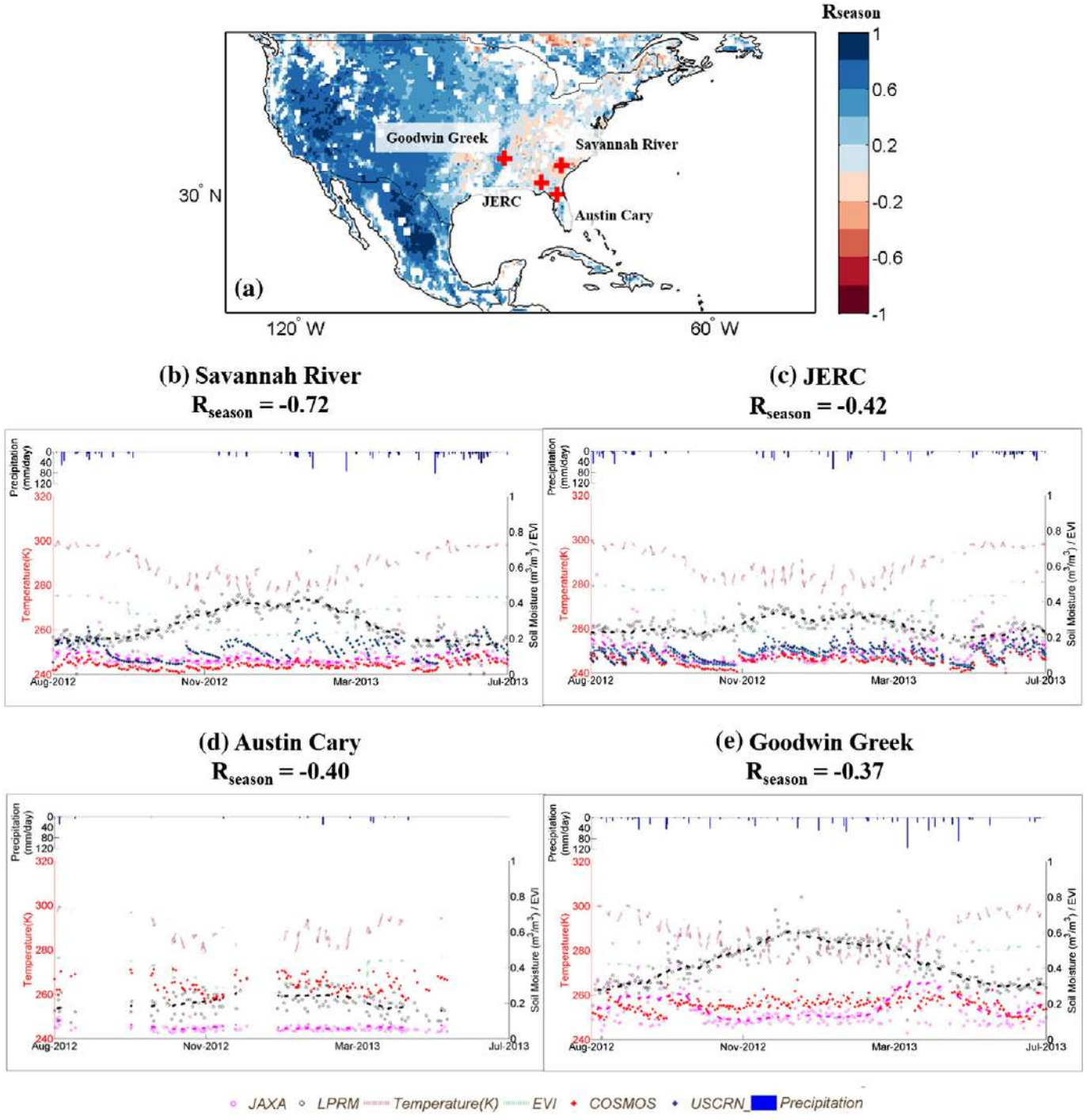

Fig. 8. Same as Fig. 7, but for four COSMOS stations where R_{season} between JAXA and LPRM product is lowest among all grid cells with COSMOS stations.

log (h) representing coarse scale surface roughness, annual mean EVI and mean value of ground soil moisture (dots in Fig. 9). It should be noted that only dates which are coincident in all datasets were used for calculating the error. To better visualize and understand the patterns in these scatterplots, smooth curves were added for each plot using robust local regression method. The regression used weighted linear least squares with a span of 50% with lower weights assigned to outliers and zero weight for data lying outside six standard deviations from the mean (lines in Fig. 9). All data used in Fig. 9 are available in Table S1. The results from this analysis are discussed in the following subsections.

3.2.1. Annual mean temperature

Biases in the JAXA product are primarily negative, which means that the values are smaller than the field measurements, whereas the LPRM product biases are generally positive. There is no significant trend in the relationship of RMSE with mean temperature for either product, although there is a sharp decrease in the correlations (R_{JAXA} and R_{LPRM}) when mean temperature decreases below 290 K. However the rate of decrease in the LPRM correlation–temperature relationship is smaller. This may be due to the large scatter in the LPRM correlation–temperature relationship compared to the JAXA case.

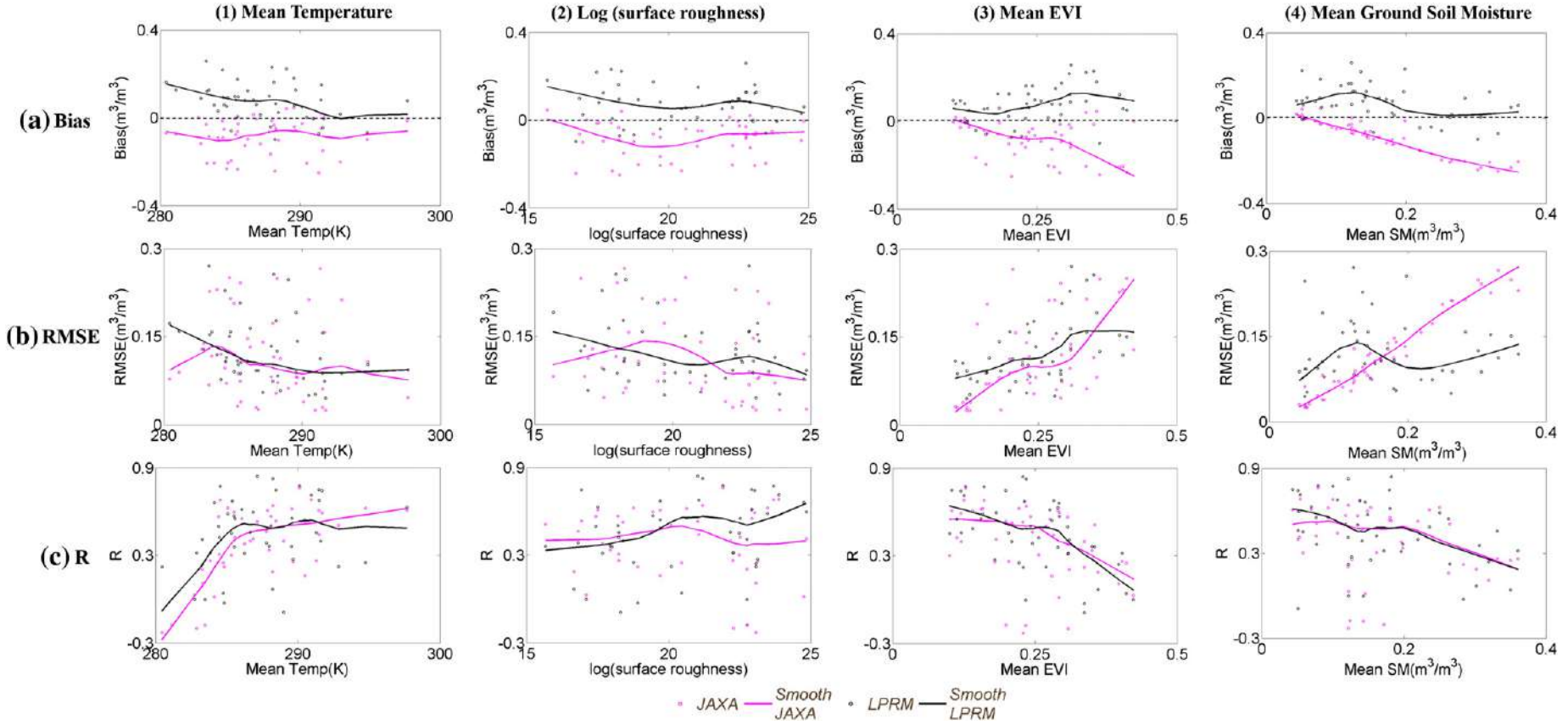

Fig. 9. Scatterplots of (y-axis) bias, RMSE and correlation coefficients (R) between AMSR2-based raw soil moisture and field measurements against (x-axis) mean temperature, coarse scale surface roughness (log (h)), mean EVI and mean ground soil moisture. A robust local regression method is used for smoothing data.

3.2.2. Surface roughness

The pattern of biases of the JAXA and LPRM products is very similar when plotted against the coarse scale surface roughness. When considering RMSE, the largest errors in the JAXA product are seen at around log (surface roughness) = 20 which is also the case for bias, while no significant trend is observed in the RMSE value of LPRM. There is a lot of scatter in the distribution of correlation coefficients against changes in log (h). However in general, there are improvements in LPRM correlations as the surface becomes rougher but JAXA correlations decrease with the rougher surface conditions. Further investigations are required to assess why LPRM correlations improved and JAXA correlations degrade with increasing surface roughness and how this knowledge could be used to improve both products.

3.2.3. Annual mean EVI

The bias in the JAXA product when considered with respect to annual mean EVI is larger than for LPRM, particularly at higher EVI values (i.e. mean EVI > 0.3).It is observed that the RMSE of JAXA increases strongly when mean EVI is higher than 0.3. The correlations of both product show a strong degradation in performance as mean EVI increases, with steeper decline in both correlation coefficients, occurring for mean EVI greater than 0.3.

3.2.4. Mean field soil moisture

There is a very clear relationship between errors in both products and mean field soil moisture. As mean field soil moisture increases the JAXA product increasingly underestimates the soil moisture (negative bias). Correlations of both products steadily decrease as mean field soil moisture increases. For LPRM, bias and RMSE are relatively constant for changes of mean field soil moisture. The exception is found for the LPRM product under dry conditions (i.e., field soil moisture < 0.2 m^3/m^3) where soil moisture is overestimated and for these sites JAXA is found to have smaller errors.

4. Discussion

The primary aim of this study is to provide guidelines for using and improving the JAXA and LPRM AMSR2 soil moisture products. In soil moisture retrieval algorithms based on the radiative transfer equation (Mo et al., 1982), it is very difficult to estimate parameters such as single scattering albedo (ω), polarization mixing ratio (Q) and roughness parameter (h) at the global scale due to the lack of experimental data to calculate them. To solve this, the parameters are generally chosen based on past research and limited site experiments (Fujii et al., 2009; Njoku & Li, 1999; Njoku et al., 2003; Owe et al., 2001). Uncertainties in the parameterizations have been used for error estimations of soil moisture retrievals (Parinussa, Meesters, et al., 2011). Although these parameterization choices will lead to biases and possible errors in the modelled dynamic ranges, it has been proved that the soil moisture retrievals generally perform well in terms of temporal variability. In many applications and particularly climate studies, the temporal variability is likely to be the most important statistics and scaling approaches have been proposed to adjust the range of soil moisture (Draper et al., 2009; Entekhabi, Reichle, Koster, & Crow, 2010; Liu, Parinussa, et al., 2011; Yilmaz & Crow, 2013). Therefore in this study we focused firstly on the temporal variability of soil moisture. Our second area of focus was to examine the difference in values resulting from the two different algorithms by using raw soil moisture retrievals. This second focus assesses the global parameterizations and suggests areas where improvements can be made in the parameterizations through improved understanding of how the two approaches affect the accuracy of soil moisture retrievals.

In the analysis, we compared two AMSR2 soil moisture products with the field soil moisture from 47 COSMOS stations. Four primary factors were identified between JAXA and LPRM retrieval algorithms, namely, physical surface temperature, surface roughness, vegetation density and quantitative soil wetness conditions, which are expected to affect the accuracy and precision of the satellite products. A summary of the performance of both products with respect to the independent variables is presented in Table 3 based on the results in Fig. 9 and discussions in the previous section. Five main conclusions are drawn. (1) The JAXA algorithm generally underestimates the ground soil moisture, whereas the LPRM algorithm tends to overestimate soil moisture. The distributions of bias and RMSE of the LPRM product are relatively insensitive to changes of the four independent variables, whereas JAXA shows larger degradations in performance above certain thresholds. (2) Correlation coefficients between AMSR2 products and ground measurements decrease when the mean temperature decreases below approximately 290 K, but the degree of decline in the LPRM product is smaller than the JAXA product. (3) Even though there is a large variance in the errors when shown against surface roughness, in general the LPRM correlations increase as the surface becomes rougher while the JAXA correlations decrease. (4) The performance of JAXA is affected in areas with dense vegetation, particularly for mean EVI greater than 0.30. Correlation coefficients of both products decline for mean EVI is higher than 0.3, which is in line with the findings in Parinussa, Meesters, et al. (2011). (5) Distributions of bias and RMSE of LPRM are relatively insensitive to variation of mean ground soil moisture; however JAXA performs better in dry condition (<0.2 m^3/m^3). Correlations for both products gradually reduce as mean ground soil moisture increases.

These results suggest possible areas for future improvement of soil moisture retrievals. Nevertheless, there are several limitations with the analyses of this study. The main factors that will have affected the results are: 1) use of data in a single year to calculate the statistics and shortage of ground stations to derive general conclusions due to the short period of data available, and 2) discrepancies in the spatial scale of AMSR2 and COSMOS soil moisture measurements.

As the AMSR2 data are made available from July 2012, its temporal coverage is less than 2 years at present. Therefore, there are not many ground stations with sufficient overlap with the study period. Secondly the short record length means that we are not able to examine inter-annual variations. Furthermore, the data mask using the 6 hourly soil temperature data reduced the number of available data. This insufficient temporal coverage and the differences in temporal resolution (i.e., hourly to monthly) like lead to more uncertainty in the results. Future research using multi-year data can potentially address this issue and provide further insights into the difference and similarity between these two AMSR2 retrieval algorithms and products.

Table 3
Summary of relative performance AMSR2-JAXA and LPRM for RMSE and correlation coefficients with mean temperature, log (h), mean EVI and mean ground soil moisture. The product with generally better results for all 47 COSMOS stations is listed. If the performance of both products was similar this is denoted by "Similar".

Variables	Range	RMSE	Correlation coefficients
Mean temp. (K)	<290	Similar	LPRM
	>290	Similar	JAXA
Log (h)	>20	[a]	LPRM
Mean EVI	<0.30	JAXA	Similar
	>0.30	LPRM	Similar
Mean ground soil moisture (m^3/m^3)	Dry (<0.20)	JAXA	Similar
	Wet (>0.20)	LPRM	Similar

[a] JAXA product shows better RMSE out of log (h) 18 to 22.

Fig. 10 shows the available number of days in common between the two datasets that can be used to calculate the correlation coefficients. Most of the ground data is located in the USA where it can be seen that there is generally a relatively low number of available records, with the number of available days decreasing as the latitude increases and the chance of freezing conditions increases, leading to more masking. Also evident in Fig. 10 is a strip across Africa, where there are extremely low numbers of days in common between the two datasets. Interestingly this effect is not evident in the ascending pass data (Fig. C4), which indicates that it is most likely due to processing of the descending pass.

The spatial resolution of the AMSR2 soil moisture is 0.25° grid and the area-averaged value over each grid represents soil moisture to a depth of a few millimetres to centimetres. On the other hand, COSMOS soil moisture is an area-representative value within a diameter of a few hundred metres and to a depth of a few hundred millimetres. For these reasons, some part of the mismatch between the AMSR2 and COSMOS soil moisture products can be attributed to these differences in horizontal and vertical support which is translated into the evaluation statistics. This is a general problem of all validation studies using in situ measurements that have different horizontal and vertical coverages compared with remotely sensed soil moisture. It is therefore appropriate to see bias and RMSE as supportive metrics showing the relative differences of the two retrievals with the reference dataset and consider correlation coefficients as the main metric.

As noted in the previous section, there is considerable scatter in the ground comparisons shown in Figs. 7, 8 and 9. This scattering issue has been reported in previous work (Draper et al., 2009). In general, this scatter has been explained by the systematic differences between the satellite-derived soil moisture and ground soil moisture. There are also uncertainties in averaging all swath data with variations due to the progression of satellite orbit, soil parameters and different spatial coverage. In this study some further possible reasons for the scatter in the relationships have been identified. First, the number of data to calculate the statistics is reduced by masking out the data under the frozen and forested conditions. Second, there are differences in the temporal resolutions of the used data (hourly to monthly).

5. Conclusions

Most previous studies validating satellite-based soil moisture products have focused on comparisons with ground data at the regional scale which have a limited range of climatic and vegetative properties, or have only considered the verification without exploring the reasons for discrepancies or good agreements. This study provides an important contribution to this area by considering global performance of the two satellite soil moisture by comparisons with ground data under various factors as well as considering the reasons for that performance.

Due to the different spatial coverage and measurement scales of the COSMOS and satellite data, the results of correlation coefficients are the most reliable. In this regard, we found that both products show rapid decreases in correlation coefficients under low mean temperature (<290 K), high mean EVI (>0.3) and highly wetted conditions. In support of these correlation results, it was found that JAXA shows relatively better performance in bias and RMSE under dry conditions, and the bias and RMSE of LPRM are generally smaller than JAXA.

The results from this study suggest areas that improvements in the algorithms could be made. Firstly, the different retrievals from the two algorithms along with the relationships of soil moisture with the four external variables (i.e. mean temperature, surface roughness, mean EVI and mean ground soil moisture) provide information on appropriate parameterizations and model selection. Another possibility is a combined product which would leverage the strengths of the JAXA and LPRM algorithms, and this would provide improvements in temporal correlations after scaling to adjust the dynamic range of the retrievals. With these, an extended work with use of a multi-year data will be conducted in the future, by which there will be more confidence in defining the seasonal cycle and the data can be decomposed to identify the anomalies where the bias is not relevant.

Supplementary data to this article can be found online at http://dx.doi.org/10.1016/j.rse.2015.02.002.

Acknowledgements

This work has been undertaken as part of a discovery project (DP140102394) funded by the Australian Research Council. The authors would like to thank the three anonymous reviewers for their helpful comments which have improved the presentation of the material and Dr. Linlin Ge for useful discussions at an early stage of the project. Yi Liu is the recipient of an Australian Research Council DECRA Fellowship (project number DE140100200). Robert Parinussa was partially funded through the European Space Agency Climate Change Initiative (584 4000104814/11/I-NB) for soil moisture (http://www.esa-soilmoisture-cci.org/). Seokhyeon Kim is funded by a University of New South Wales Tuition Fee Scholarship (TFS). The authors would also like to thank JAXA for making AMSR2 data available online.

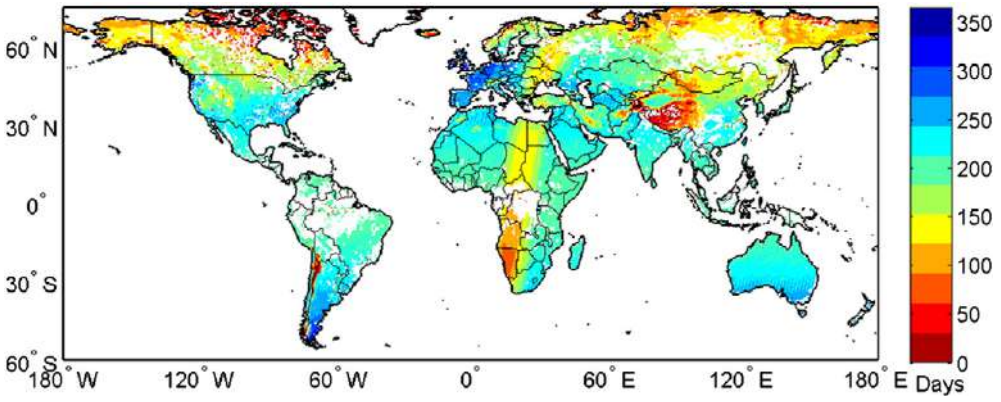

Fig. 10. Number of days available to calculate correlations between JAXA and LPRM soil moisture estimates.

Appendix A. Global map of paired t-test results for descending data

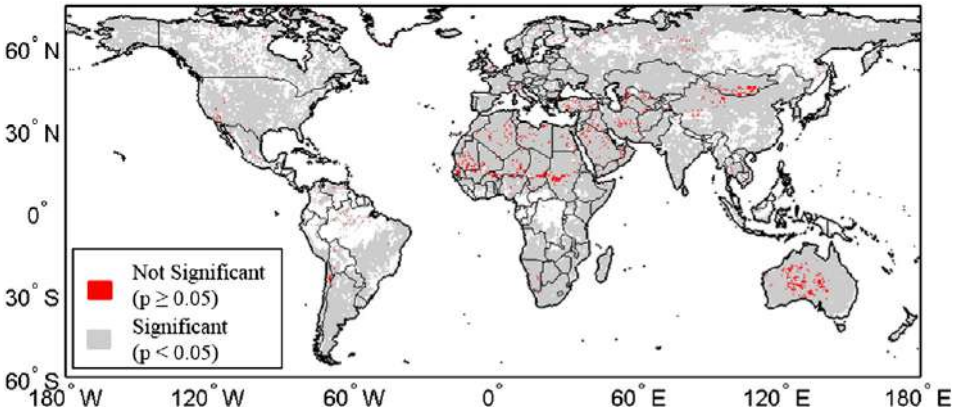

Fig. A1. Global map (descending) of p values from a paired t-test for a null hypothesis, $\mu_{JAXA} = \mu_{LPRM}$ with $\alpha = 0.05$. Over the desert regions, soil moisture values from both AMSR2 products are consistently low during the entire year, and their difference is very small and not statistically significant.

Appendix B. Global map of coarse scale surface roughness

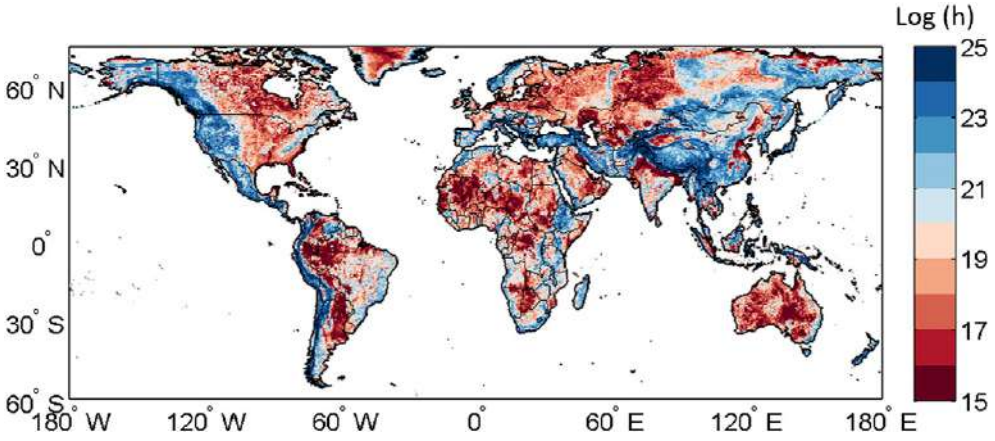

Fig. B1. Global map of coarse scale surface roughness (log (h)) derived from 1-km DEM.

Appendix C. Results for ascending data

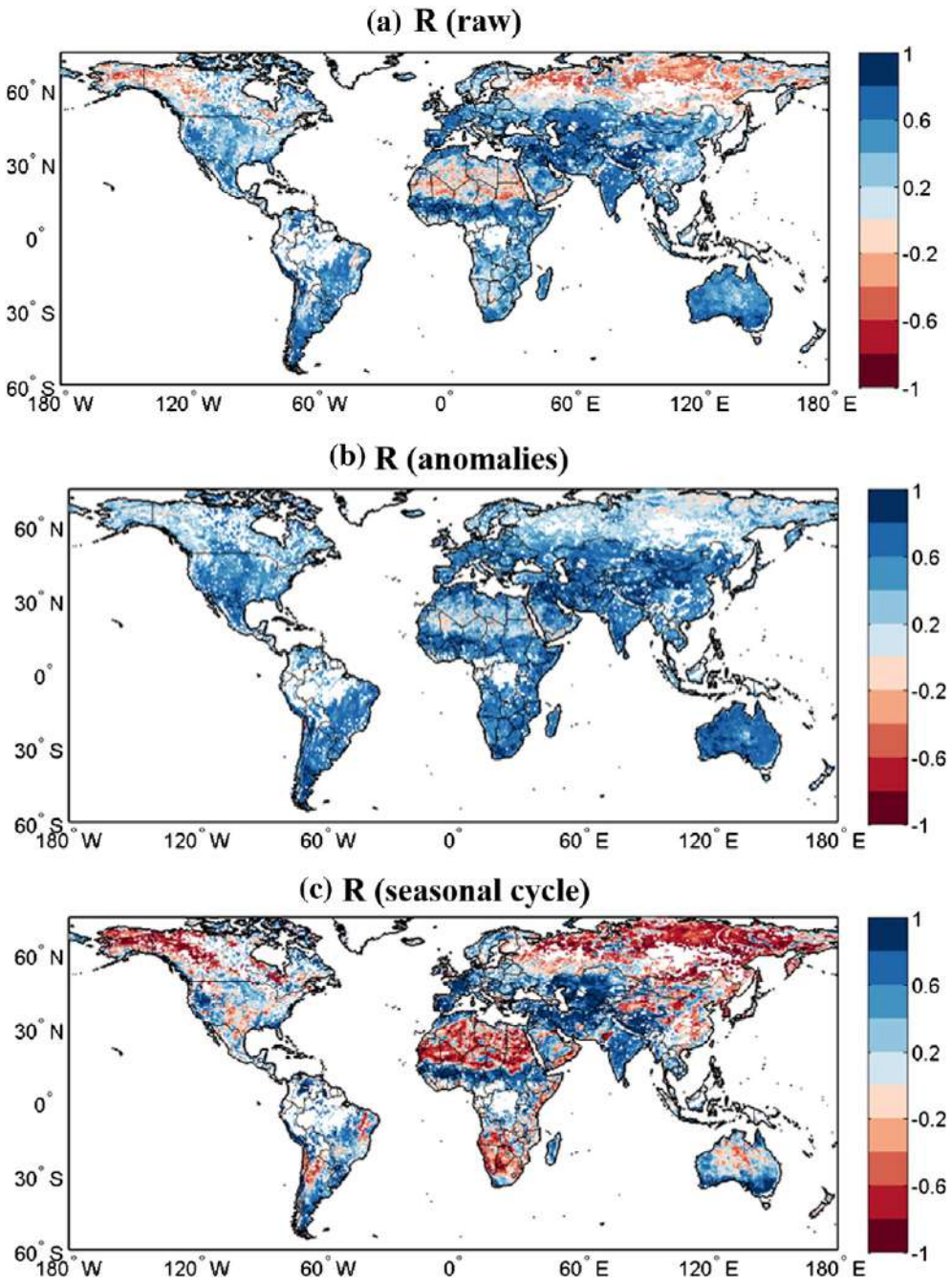

Fig. C1. Global maps of correlation coefficients (R) between JAXA and LPRM soil moisture products derived from ascending overpasses of 10.7 GHz (X-band) for the period 01/08/2012 to 31/07/2013. (a) Raw soil moisture (R_{raw}), (b) anomalies ($R_{anomaly}$) and (c) seasonal cycle (R_{season}).

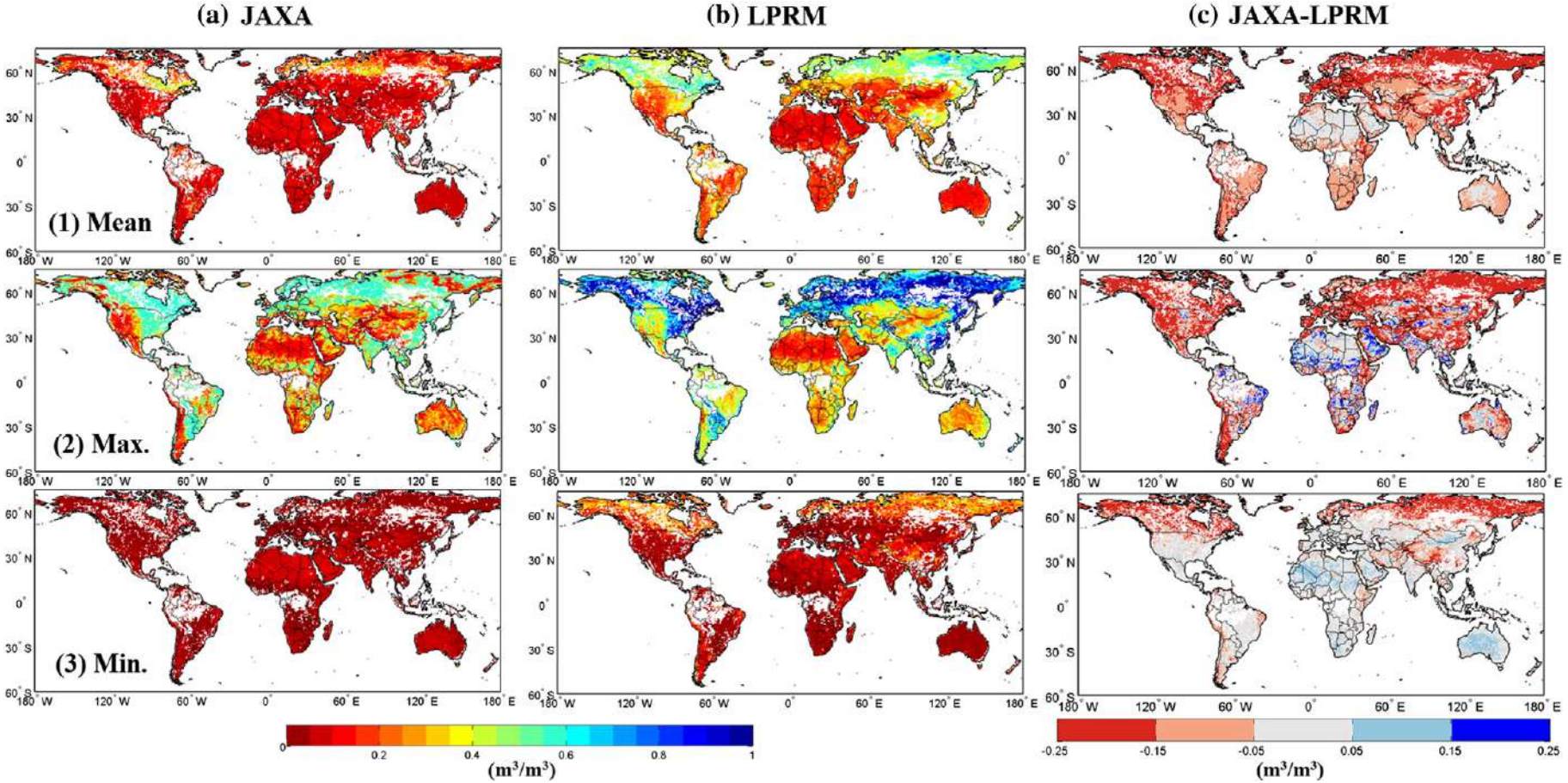

Fig. C2. Global maps of mean (top panels), maximum (middle panels) and minimum (bottom panels) values of JAXA (left column), LPRM (middle column) and differences (i.e., JAXA–LPRM, right column) derived from ascending overpasses.

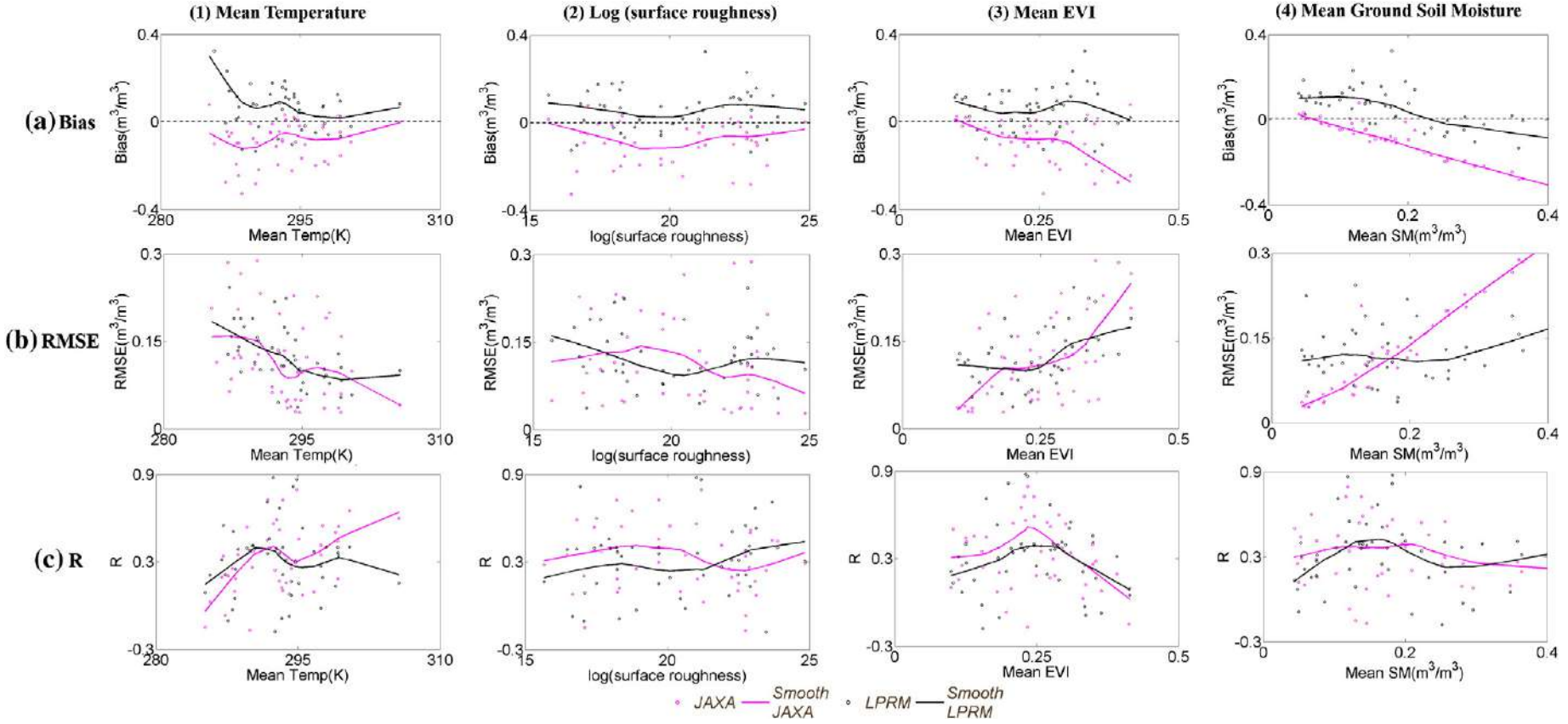

Fig. C3. Scatterplots of (y-axis) bias, RMSE and correlation coefficients (R) between AMSR2-based soil moisture and ground-based measurements against (x-axis) mean temperature, roughness (log (h)), mean EVI and mean ground soil moisture. A robust local regression method is used for smoothing data.

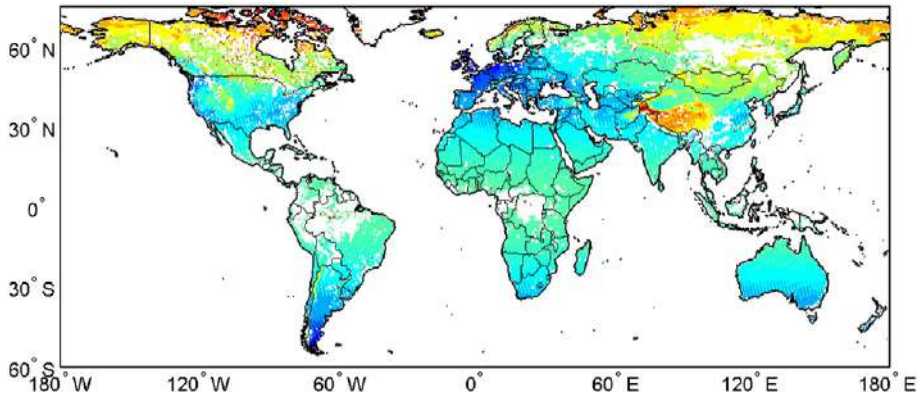

Fig. C4. Number of available days to calculate correlations between JAXA soil moisture and LPRM soil moisture based on ascending data and p values indicating the significance of correlation coefficients.

References

Albergel, C., de Rosnay, P., Gruhier, C., Muñoz-Sabater, J., Hasenauer, S., Isaksen, L., et al. (2012). Evaluation of remotely sensed and modelled soil moisture products using global ground-based in situ observations. *Remote Sensing of Environment*, *118*, 215–226.

Albergel, C., Dorigo, W., Balsamo, G., Muñoz-Sabater, J., de Rosnay, P., Isaksen, L., et al. (2013). Monitoring multi-decadal satellite earth observation of soil moisture products through land surface reanalyses. *Remote Sensing of Environment*, *138*(0), 77–89. http://dx.doi.org/10.1016/j.rse.2013.07.009.

Al-Yaari, A., Wigneron, J.P., Ducharne, A., Kerr, Y., de Rosnay, P., de Jeu, R., et al. (2014). Global-scale evaluation of two satellite-based passive microwave soil moisture datasets (SMOS and AMSR-E) with respect to Land Data Assimilation System estimates. *Remote Sensing of Environment*, *149*(0), 181–195. http://dx.doi.org/10.1016/j.rse.2014.04.006.

Becker, F., & Choudhury, B.J. (1988). Relative sensitivity of normalized difference vegetation index (NDVI) and microwave polarization difference index (MPDI) for vegetation and desertification monitoring. *Remote Sensing of Environment*, *24*(2), 297–311.

Bogena, H.R., Huisman, J.A., Baatz, R., Hendricks Franssen, H.J., & Vereecken, H. (2013). Accuracy of the cosmic-ray soil water content probe in humid forest ecosystems: The worst case scenario. *Water Resources Research*, *49*(9), 5778–5791. http://dx.doi.org/10.1002/wrcr.20463.

Brocca, L., Hasenauer, S., Lacava, T., Melone, F., Moramarco, T., Wagner, W., et al. (2011). Soil moisture estimation through ASCAT and AMSR-E sensors: An intercomparison and validation study across Europe. *Remote Sensing of Environment*, *115*(12), 3390–3408.

Brocca, L., Melone, F., Moramarco, T., Wagner, W., Naeimi, V., Bartalis, Z., et al. (2010). Improving runoff prediction through the assimilation of the ASCAT soil moisture product. *Hydrology and Earth System Sciences*, *14*(10), 1881–1893. http://dx.doi.org/10.5194/hess-14-1881-2010.

Bruckler, L., & Witono, H. (1989). Use of remotely sensed soil moisture content as boundary conditions in soil-atmosphere water transport modeling: 2. Estimating soil water balance. *Water Resources Research*, *25*(12), 2437–2447.

Chen, F., Crow, W.T., Starks, P.J., & Moriasi, D.N. (2011). Improving hydrologic predictions of a catchment model via assimilation of surface soil moisture. *Advances in Water Resources*, *34*(4), 526–536. http://dx.doi.org/10.1016/j.advwatres.2011.01.011.

Choudhury, B.J., Schmugge, T.J., Chang, A., & Newton, R.W. (1979). Effect of surface roughness on the microwave emission from soils. *Journal of Geophysical Research, Oceans*, *84*(C9), 5699–5706. http://dx.doi.org/10.1029/JC084iC09p05699.

Crow, W.T., Miralles, D.G., & Cosh, M.H. (2010). A quasi-global evaluation system for satellite-based surface soil moisture retrievals. *IEEE Transactions on Geoscience and Remote Sensing*, *48*(6), 2516–2527. http://dx.doi.org/10.1109/TGRS.2010.2040481.

Crow, W.T., & Ryu, D. (2009). A new data assimilation approach for improving runoff prediction using remotely-sensed soil moisture retrievals. *Hydrology and Earth System Sciences*, *13*(1), 1–16. http://dx.doi.org/10.5194/hess-13-1-2009.

De Jeu, R.A.M., & Owe, M. (2003). Further validation of a new methodology for surface moisture and vegetation optical depth retrieval. *International Journal of Remote Sensing*, *24*(22), 4559–4578. http://dx.doi.org/10.1080/0143116031000095934.

De Jeu, R.A.M., Wagner, W., Holmes, T.R.H., Dolman, A.J., Giesen, N.C., & Friesen, J. (2008). Global soil moisture patterns observed by space borne microwave radiometers and scatterometers. *Surveys in Geophysics*, *29*(4–5), 399–420. http://dx.doi.org/10.1007/s10712-008-9044-0.

Dee, D.P., Uppala, S.M., Simmons, A.J., Berrisford, P., Poli, P., Kobayashi, S., et al. (2011). The ERA-Interim reanalysis: Configuration and performance of the data assimilation system. *Quarterly Journal of the Royal Meteorological Society*, *137*(656), 553–597. http://dx.doi.org/10.1002/qj.828.

Diamond, H.J., Karl, T.R., Palecki, M.A., Baker, C.B., Bell, J.E., Leeper, R.D., et al. (2013). U.S. climate reference network after one decade of operations: Status and assessment. *Bulletin of the American Meteorological Society*, *94*(4), 485–498. http://dx.doi.org/10.1175/BAMS-D-12-00170.1.

Dorigo, W.A., Scipal, K., Parinussa, R.M., Liu, Y.Y., Wagner, W., de Jeu, R.A.M., et al. (2010). Error characterisation of global active and passive microwave soil moisture datasets. *Hydrology and Earth System Sciences*, *14*(12), 2605–2616. http://dx.doi.org/10.5194/hess-14-2605-2010.

Dorigo, W.A., Wagner, W., Hohensinn, R., Hahn, S., Paulik, C., Xaver, A., et al. (2011). The International Soil Moisture Network: A data hosting facility for global in situ soil moisture measurements. *Hydrology and Earth System Sciences*, *15*(5), 1675–1698. http://dx.doi.org/10.5194/hess-15-1675-2011.

Dorigo, W., Xaver, A., Vreugdenhil, M., Gruber, A., Hegyiová, A., Sanchis-Dufau, A., et al. (2013). Global automated quality control of in situ soil moisture data from the International Soil Moisture Network. *Vadose Zone Journal*, *12*(3).

Draper, C.S., Walker, J.P., Steinle, P.J., De Jeu, R.A.M., & Holmes, T.R.H. (2009). An evaluation of AMSR-E derived soil moisture over Australia. *Remote Sensing of Environment*, *113*(4), 703–710.

Engman, E.T. (1991). Applications of microwave remote sensing of soil moisture for water resources and agriculture. *Remote Sensing of Environment*, *35*(2), 213–226.

Entekhabi, D., Reichle, R.H., Koster, R.D., & Crow, W.T. (2010). Performance metrics for soil moisture retrievals and application requirements. *Journal of Hydrometeorology*, *11*(3).

Fujii, H., Koike, T., & Imaoka, K. (2009). Improvement of the AMSR-E algorithm for soil moisture estimation by introducing a fractional vegetation coverage dataset derived from MODIS data. *Journal of the Remote Sensing Society of Japan*, *29*(1), 11.

GLOBE-Task-Team, et al. (1999). The Global Land One-kilometer Base Elevation (GLOBE) Digital Elevation Model, Version 1.0. Retrieved from: http://www.ngdc.noaa.gov/mgg/topo/globe.html

Gruhier, C., de Rosnay, P., Hasenauer, S., Holmes, T., de Jeu, R., Kerr, Y., et al. (2010). Soil moisture active and passive microwave products: Intercomparison and evaluation over a Sahelian site. *Hydrology and Earth System Sciences*, *14*(1), 141–156.

Hain, C.R., Crow, W.T., Mecikalski, J.R., Anderson, M.C., & Holmes, T. (2011). An intercomparison of available soil moisture estimates from thermal infrared and passive microwave remote sensing and land surface modeling. *Journal of Geophysical Research, [Atmospheres]*, *116*(D15), D15107. http://dx.doi.org/10.1029/2011JD015633.

Huffman, G. J., & Bolvin, D. T. (2014). TRMM and other data precipitation data set documentation. From ftp://precip.gsfc.nasa.gov/pub/trmmdocs/3B42_3B43_doc.pdf

Imaoka, K., Kachi, M., Kasahara, M., Ito, N., Nakagawa, K., & Oki, T. (2010). Instrument performance and calibration of AMSR-E and AMSR2. *The International Archives of the Photogrammetry, Remote Sensing and Spatial Information Sciences*, *38*(Part 8).

Jackson, T.J. (1993). III. Measuring surface soil moisture using passive microwave remote sensing. *Hydrological Processes*, *7*(2), 139–152.

Jackson, T.J., Cosh, M.H., Bindlish, R., Starks, P.J., Bosch, D.D., Seyfried, M., et al. (2010). Validation of advanced microwave scanning radiometer soil moisture products. *IEEE Transactions on Geoscience and Remote Sensing*, *48*(12), 4256–4272. http://dx.doi.org/10.1109/TGRS.2010.2051035.

Jackson, T. J., & Schmugge, T. J. (1991). *Vegetation effects on the microwave emission of soils.*

Jackson, T.J., Schmugge, J., & Engman, E.T. (1996). Remote sensing applications to hydrology: Soil moisture. *Hydrological Sciences Journal-Journal Des Sciences Hydrologiques*, *41*(4), 517–530. http://dx.doi.org/10.1080/02626669609491523.

Koike, T. (2013). *Soil moisture algorithm descriptions of GCOM-W1 AMSR2 (Rev. A).* Earth Observation Research Center, Japan Aerospace Exploration Agency, 8-1–8-13 Retrieved from http://suzaku.eorc.jaxa.jp/GCOM_W/data/doc/NDX-120015A.pdf.

Koike, T., Nakamura, Y., Kaihotsu, I., Davva, G., Matsuura, N., Tamagawa, K., et al. (2004). Development of an advanced microwave scanning radiometer (AMSR-E) algorithm of soil moisture and vegetation water content. *Annual Journal of Hydraulic Engineering, JSCE*, *48*(2), 6.

Koike, T., Tsukamoto, T., Kumakura, T., & Lu, M. (1996). Spatial and seasonal distribution of surface wetness derived from satellite data. *Paper presented at the Proceeding of the International Workshop on Macro-Scale Hydrological Modeling.*

Koster, R.D., Dirmeyer, P.A., Guo, Z., Bonan, G., Chan, E., Cox, P., et al. (2004). Regions of strong coupling between soil moisture and precipitation. *Science*, *305*(5687), 1138–1140.

Liu, G. (1998). A fast and accurate model for microwave radiance calculations. *Journal of the Meteorological Society of Japan*, *76*(2), 335–343.

Liu, Y.Y., de Jeu, R.A., McCabe, M.F., Evans, J.P., & van Dijk, A.I. (2011a). Global long-term passive microwave satellite-based retrievals of vegetation optical depth. *Geophysical Research Letters*, *38*(18).

Liu, Y.Y., Parinussa, R.M., Dorigo, W.A., De Jeu, R.A.M., Wagner, W., van Dijk, A.I.J.M., et al. (2011b). Developing an improved soil moisture dataset by blending passive and active microwave satellite-based retrievals. *Hydrology and Earth System Sciences*, *15*(2), 425–436. http://dx.doi.org/10.5194/hess-15-425-2011.

Liu, Y.Y., van Dijk, A.I.J.M., McCabe, M.F., Evans, J.P., & de Jeu, R.A.M. (2013). Global vegetation biomass change (1988–2008) and attribution to environmental and human drivers. *Global Ecology and Biogeography*, *22*(6), 692–705. http://dx.doi.org/10.1111/geb.12024.

Meesters, A.G.C.A., De Jeu, R.A.M., & Owe, M. (2005). Analytical derivation of the vegetation optical depth from the microwave polarization difference index. *IEEE Geoscience and Remote Sensing Letters*, *2*(2), 121–123.

Miralles, D.G., Crow, W.T., & Cosh, M.H. (2010). Estimating spatial sampling errors in coarse-scale soil moisture estimates derived from point-scale observations. *Journal of Hydrometeorology*, *11*(6), 1423–1429. http://dx.doi.org/10.1175/2010JHM1285.1.

Mo, T., Choudhury, B.J., Schmugge, T.J., Wang, J.R., & Jackson, T.J. (1982). A model for microwave emission from vegetation-covered fields. *Journal of Geophysical Research, Oceans*, *87*(C13), 11229–11237. http://dx.doi.org/10.1029/JC087iC13p11229.

Njoku, E.G., Ashcroft, P., Chan, T.K., & Li, L. (2005). Global survey and statistics of radio-frequency interference in AMSR-E land observations. *IEEE Transactions on Geoscience and Remote Sensing*, *43*(5), 938–947.

Njoku, E.G., & Entekhabi, D. (1996). Passive microwave remote sensing of soil moisture. *Journal of Hydrology*, *184*(1–2), 101–129. http://dx.doi.org/10.1016/0022-1694(95)02970-2.

Njoku, E.G., Jackson, T.J., Lakshmi, V., Chan, T.K., & Nghiem, S.V. (2003). Soil moisture retrieval from AMSR-E. *IEEE Transactions on Geoscience and Remote Sensing*, *41*(2), 215–229. http://dx.doi.org/10.1109/TGRS.2002.808243.

Njoku, E.G., Koike, T., Jackson, T., & Paloscia, S. (1999). *Retrieval of soil moisture from AMSR data. Microwave radiometry for remote sensing of the earth's surface and atmosphere*, *9*, Netherlands: VSP Publishing.

Njoku, E.G., & Li, L. (1999). Retrieval of land surface parameters using passive microwave measurements at 6–18 GHz. *IEEE Transactions on Geoscience and Remote Sensing*, *37*(1), 79–93.

Owe, M., De Jeu, R.A.M., & Holmes, T. (2008). Multisensor historical climatology of satellite-derived global land surface moisture. *Journal of Geophysical Research, Earth Surface*, *113*(F1), F01002. http://dx.doi.org/10.1029/2007JF000769.

Owe, M., De Jeu, R.A.M., & Walker, J. (2001). A methodology for surface soil moisture and vegetation optical depth retrieval using the microwave polarization difference index. *IEEE Transactions on Geoscience and Remote Sensing*, *39*(8), 1643–1654. http://dx.doi.org/10.1109/36.942542.

Paloscia, S., Macelloni, G., & Santi, E. (2006). Soil moisture estimates from AMSR-E brightness temperatures by using a dual-frequency algorithm. *IEEE Transactions on Geoscience and Remote Sensing*, *44*(11), 3135–3144. http://dx.doi.org/10.1109/TGRS.2006.881714.

Paloscia, S., & Pampaloni, P. (1988). Microwave polarization index for monitoring vegetation growth. *IEEE Transactions on Geoscience and Remote Sensing*, *26*(5), 617–621. http://dx.doi.org/10.1109/36.7687.

Parinussa, R., Holmes, T., Wanders, N., Dorigo, W., & de Jeu, R. (2015). A Preliminary Study Towards Consistent Soil Moisture from AMSR2. *J. Hydrometeor*. http://dx.doi.org/10.1175/JHM-D-13-0200.1 (in press).

Parinussa, R., Holmes, T., Yilmaz, M., & Crow, W. (2011). The impact of land surface temperature on soil moisture anomaly detection from passive microwave observations. *Hydrology and Earth System Sciences*, *15*(10), 3135–3151.

Parinussa, R.M., Meesters, A.G.C.A., Liu, Y., Dorigo, W., Wagner, W., & De Jeu, R.A.M. (2011). Error estimates for near-real-time satellite soil moisture as derived from the land parameter retrieval model. *IEEE Geoscience and Remote Sensing Letters*, *8*(4), 779–783.

Rosolem, R., Shuttleworth, W.J., Zreda, M., Franz, T.E., Zeng, X., & Kurc, S.A. (2013). The effect of atmospheric water vapor on neutron count in the cosmic-ray soil moisture observing system. *Journal of Hydrometeorology*, *14*(5), 1659–1671. http://dx.doi.org/10.1175/JHM-D-12-0120.1.

Schmugge, T.J., Kustas, W.P., Ritchie, J.C., Jackson, T.J., & Rango, A. (2002). Remote sensing in hydrology. *Advances in Water Resources*, *25*(8–12), 1367–1385. http://dx.doi.org/10.1016/S0309-1708(02)00065-9.

Scipal, K., Holmes, T., de Jeu, R., Naeimi, V., & Wagner, W. (2008). A possible solution for the problem of estimating the error structure of global soil moisture data sets. *Geophysical Research Letters*, *35*(24), L24403. http://dx.doi.org/10.1029/2008GL035599.

Wagner, W., Bloschl, G., Pampaloni, P., Calvet, J. -C., Bizzarri, B., Wigneron, J. -P., et al. (2007). Operational readiness of microwave remote sensing of soil moisture for hydrologic applications. *Nordic Hydrology*, *38*(1), 1–20.

Wang, J. R., & Schmugge, T. J. (1980). An Empirical Model for the Complex Dielectric Permittivity of Soils as a Function of Water Content. *Geoscience and Remote Sensing, IEEE Transactions on*, *GE-18*(4), 288–295. http://dx.doi.org/10.1109/TGRS.1980.350304.

Wigneron, J., Chanzy, A., Calvet, J., & Bruguier, N. (1995). A simple algorithm to retrieve soil moisture and vegetation biomass using passive microwave measurements over crop fields. *Remote Sensing of Environment*, *51*(3), 331–341.

Wigneron, J., Schmugge, T.J., Chanzy, A., Calvet, J., & Kerr, Y. (1998). Use of passive microwave remote sensing to monitor soil moisture. *Agronomie*, *18*(1), 27–43.

Yee, M., Walker, J.P., Dumedah, G., Monerris, A., & Rüdiger, C. (2013). Towards land surface model validation from using satellite retrieved soil moisture. *Paper presented at the 20th International Congress on Modelling and Simulation, Adelaide, Australia*.

Yilmaz, M.T., & Crow, W.T. (2013). The optimality of potential rescaling approaches in land data assimilation. *Journal of Hydrometeorology*, *14*(2).

Zhu, H.D., Shi, Z.H., Fang, N.F., Wu, G.L., Guo, Z.L., & Zhang, Y. (2014). Soil moisture response to environmental factors following precipitation events in a small catchment. *Catena*, *120*(0), 73–80. http://dx.doi.org/10.1016/j.catena.2014.04.003.

Zreda, M., Shuttleworth, W., Zeng, X., Zweck, C., Desilets, D., Franz, T., et al. (2012). COSMOS: the COsmic-ray Soil Moisture Observing System. *Hydrology and Earth System Sciences*, *16*(11).